

**Frequentists and Bayesian methods to incorporate
recruitment rate stochasticity
at the design stage of a clinical trial**

Master Thesis in Biostatistics (STA495)

by

Pilar Pastor Martinez
23-733-975

supervised by

PD Dr. Malgorzata Roos

Zurich, June 2025

Frequentists and Bayesian methods to incorporate recruitment rate stochasticity at the design stage of a clinical trial

Pilar Pastor Martinez

Version May 28, 2025

Contents

Acknowledgements	iii
Abstract	1
1 Introduction	3
2 Background	5
2.1 Definitions	5
2.2 Uncertainty and models for counts and time	6
3 Methods for Counts	9
3.1 Counts: Model based on Expectations	9
3.2 Counts: Model based on Poisson Process	10
3.3 Counts: Negative Binomial model derived from Poisson-Gamma model	11
3.4 Comparison of models for the accrual of counts	20
3.5 Generation of Poisson-Gamma model	20
4 Methods for Waiting Time	27
4.1 Time: Model based on Expectations	27
4.2 Time: Model based on Erlang distribution	27
4.3 Time: Derivation of Gamma-Gamma model	27
5 Results	33
5.1 Example from Carter	33
5.2 Pros and cons of Monte Carlo simulations	33
5.3 Important questions when forecasting recruitment at the design-stage of a study	33
5.4 Counts: Comparison exact vs Monte Carlo simulations	34
5.5 Time: Comparison exact vs Monte Carlo simulations	34
6 Discussion	41
A Reproducibility	43
A.1 Code Availability	43
A.2 Personal Statement	43

A.3 Session Info	43
Bibliography	45

Acknowledgements

I am profoundly grateful to my supervisor, PD Dr. Malgorzata Roos, whose expert guidance and steadfast support were instrumental in the completion of this thesis. Her insightful feedback, dedication, and genuine enthusiasm for my research provided both direction and motivation throughout this process. I also thank the faculty of the Biostatistics Master's Program for providing a strong academic foundation and a challenging learning environment that contributed significantly to my development.

Pilar Pastor Martinez
Zurich, June 2025

Abstract

In clinical trials, inaccurate or overly optimistic projections of recruitment rates can lead to the failure of enrolling a sufficient number of patients within the required time frame. This can ultimately result in study discontinuation, delays, or inconclusive statistical findings. In practice, many researchers rely on deterministic models that do not adequately capture the stochasticity inherent in the patient recruitment process. While more sophisticated exact stochastic methods exist, they often use simulations, which can yield approximate estimates of trial duration. These limitations highlight the need for exact methods for predicting recruitment timelines and accrual. To address this gap, we developed exact statistical methods that account for both aleatory uncertainty (stemming from random variability) and epistemic uncertainty (due to lack of knowledge about the true recruitment rate). To support the implementation of the methods, visualizations of patient leakage and a unified mathematical notation were developed. For modeling the number of patients recruited over time (T_{target}), we use Poisson and Poisson-Gamma models, while for waiting times until a certain number of patients is recruited (C_{target}), we apply Erlang and Gamma-Gamma approach. These developments are supported by open source Software provided on GitHub. These exact models allow for more accurate predictions of the time needed to reach a desired sample size. This provides a more reliable basis for planning clinical trials, allocating resources, and setting expectations on realistic recruitment. By integrating uncertainty more thoroughly, our approach enhances the transparency and credibility of trial planning and supports better-informed decision-making in clinical research.

Chapter 1

Introduction

At the design stage of a clinical trial researchers develop the trial protocol, determine the study population and define objectives. Accurate statistical analysis at the end of a trial require an adequate number of observations to draw valid and reliable conclusions (Panos and Boeckler, 2023). These observations (C_{target}) are specified by the optimal sample size computation to show a relevant effect. However, the study duration in which these patients ought to be recruited (T_{target}) is often limited by funding. As such, reliable recruitment projections at the design stage are essential for all areas of scientific research. Inaccurate or overly optimistic projections can lead to studies failing to collect enough data within the required time frame, potentially resulting in study discontinuation or inconclusive statistical results.

The Design-Stage Recruitment Analysis (DSRA), as described by Carter (2004), involves predicting the number of participants expected to be recruited by a specified future time point, as well as estimating the waiting time required to reach a predetermined target number of observations. Carter’s approach models recruitment using a Poisson process with a fixed rate, employing Monte Carlo (MC) simulations to account solely for aleatory uncertainty (O’Hagan, 2006). In contrast, more advanced methods - such as the exact approach by Anisimov and Fedorov (2007) or the Bayesian method proposed by Bagiella and Heitjan (2001) - address both aleatory and epistemic uncertainty (O’Hagan, 2006), by allowing the recruitment rate to vary. The aim of this Master’s thesis is to evaluate whether Carter’s method can be improved and extended to incorporate these additional sources of uncertainty.

Chapter 2 presents a generalized framework for the stages of a clinical trial, inspired by a real CONSORT study flow diagram (Schulz *et al.*, 2010; Hopewell *et al.*, 2025). Each stage is clearly defined, with particular attention given to patient leakage between stages (Desai, 2014). This chapter also introduces the concept of recruitment rate and distinguishes between two types of uncertainty: aleatory and epistemic (O’Hagan, 2006). Chapters 3 and 4 detail the methodological approaches for predicting participant counts and recruitment times, respectively. These range from deterministic models, which assume no uncertainty, to more sophisticated exact methods that incorporate both aleatory and epistemic uncertainty. Both chapters include sensitivity analyses and summary tables reporting statistical moments and measures of uncertainty. Finally, Chapter 5 applies the exact methods developed in the preceding chapters to a real clinical trial (Carter, 2004), compares them with corresponding Monte Carlo simulations, and evaluates their reliability. A link to the Open Source R Software is provided in the Appendix A.

Chapter 2

Background

2.1 Definitions

The general notion of **Recruitment** in this Master Thesis refers to the number of patients (Counts) at the Eligibility, or Enrollment, or Randomization, or Statistical Analysis stage in Figure 2.1. Figure 2.1 is a schematic representation of a CONSORT study flow chart (Schulz *et al.*, 2010; Hopewell *et al.*, 2025) inspired by a real CONSORT study flow chart in Figure 2.2. We define **Accrual** as cumulative recruitment.

The **Target Population** is a specific group within the broader population, defined by attributes relevant to the research question. This group is focused on criteria that match the study's goals (Willie, 2024). Defining the target population allows researchers to refine their objectives and recruitment methods to align with the study's aims.

The **Eligibility** criteria are the specific requirements that individuals must meet to participate in a study. Eligible patients will be selected from the target population. Inclusion criteria specify the conditions that allow individuals to participate in the trial, particularly focusing on the medical condition of interest. Any other factors that limit eligibility are classified as exclusion criteria (Van Spall *et al.*, 2007), conditions or circumstances that disqualify potential participants (Food *et al.*, 2018).

In clinical trials, **Enrollment** refers to the formal process of registering participants into a study after they have met all eligibility criteria and provided informed consent. This process includes verifying that each participant satisfies the inclusion and exclusion criteria outlined in the study protocol (National Institute of Allergy and Infectious Diseases, 2021). It is important to distinguish between recruitment and enrollment. Recruitment involves identifying and inviting potential participants to join the study, whereas enrollment occurs after these individuals have been screened, consented, and officially registered into the trial (Frank, 2004).

Once enrolled, participants are assigned to specific treatment groups or interventions as defined by the study design. The most common practice is **Randomization**. In clinical research, randomization is the process of assigning participants to different treatment groups using chance methods, such as random number generators or coin flips (Lim and In, 2019). Randomized controlled trials (RCTs) are considered the most effective method for preventing bias in the evaluation of new interventions, drugs, or devices. (Van Spall *et al.*, 2007).

In clinical research, **Statistical Analysis** involves applying statistical methods to collect, summarize, interpret, and present data derived from clinical studies. This process is essential for evaluating the safety, efficacy, and overall outcomes of medical interventions, ensuring that conclusions drawn are both reliable and valid (Panos and Boeckler, 2023). Not all participants who are randomized may be included in the final statistical analysis due to protocol deviations of patients not adhering to the protocol (Rehman *et al.*, 2020), missing data (Shih, 2002) or loss-to-follow-up, some participants may become unreachable or withdraw consent during the study, resulting in missing outcome data (Nüesch *et al.*, 2009).



Figure 2.1: Patient recruitment and leakage at each stage of a clinical study (Piantadosi and Meinert, 2022; Whelan *et al.*, 2018; Bogin, 2022).

The number of patients decreases at each stage of a clinical study, from defining the target population to final statistical analysis, see Figure 2.3. This process is known as patient leakage (Desai, 2014), alternative terms are attrition or retention.

Figure 2.1 generalizes the notion of patient leakage found in trial profiles such as the one found in Figure 2.2. Figure 2.1 outlines the various stages of a clinical trial and analyzes the key factors contributing to patient attrition as they transition from one stage to the next.

Eligibility criteria narrow down participants, and enrollment further reduces numbers as only those meeting strict criteria are registered. Randomization assigns individuals to treatment groups, but some may later be excluded due to protocol deviations, missing data, or loss to follow-up.

2.2 Uncertainty and models for counts and time

There are two types of uncertainty, aleatory and epistemic (O’Hagan, 2006). The **Aleatory Uncertainty** reflects randomness that is inherent, irreducible and unpredictable in nature. **Epistemic Uncertainty** arises primarily from limited or imperfect knowledge about the parameters of a statistical model and can reflect fluctuations of the parameter. Obtaining more or better information about the parameter typically reduces the epistemic uncertainty.

Let us denote

- $T = \text{time}$
- $C = \text{counts}$
- $\lambda = \frac{C}{T}$

We define **Recruitment Rate** $\lambda = \frac{C}{T}$ at which patients are collected, measured as persons per unit of time, where **Rate** is understood as a ratio in which the numerator and denominator are incremental differences (Piantadosi, 2024):

$$\lambda = \frac{\Delta C}{\Delta T} = \frac{C_1 - C_0}{T_1 - T_0} = \frac{C_1 - 0}{T_1 - 0} = \frac{C_1}{T_1}$$

Methods in Tables 3.1, 3.2 and 4.1 are applicable to each level of recruitment in Figures 2.1 and 2.3.

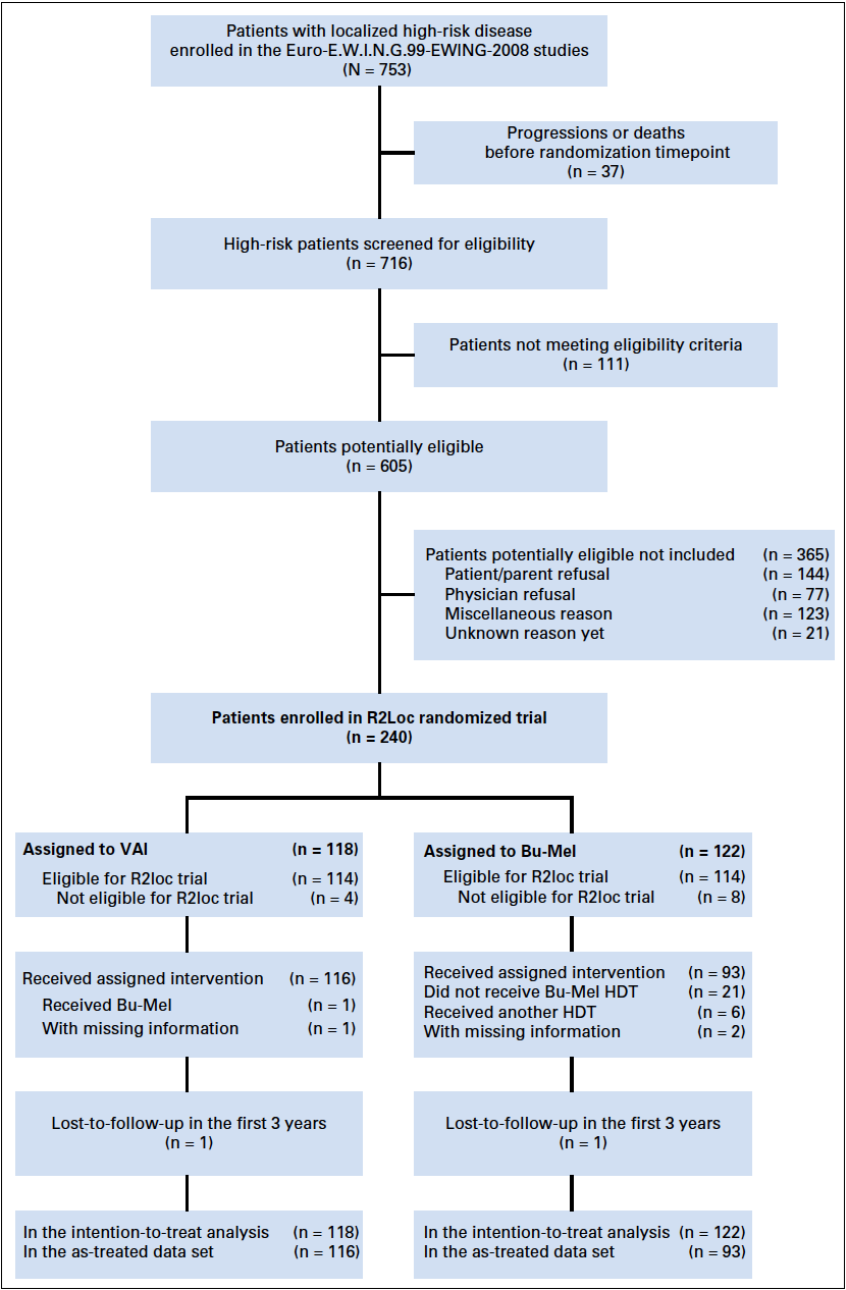


Figure 2.2: CONSORT study flow-chart (Whelan *et al.*, 2018; Schulz *et al.*, 2010; Hopewell *et al.*, 2025).



Figure 2.3: Visual representation of patient recruitment and leakage at each stage of a clinical study (Piantadosi and Meinert, 2022; Whelan *et al.*, 2018; Bogin, 2022).

Chapter 3

Methods for Counts

3.1 Counts: Model based on Expectations

If we fix the duration of a study at time T and we expect that we collect C patients until T , we deterministically predict the recruitment rate per one unit of time (without taking into consideration any uncertainty) to be $\hat{\lambda} = \frac{C}{T}$ (Carter, 2004).

3.1.1 Expected recruitment in one unit of time

Assume that the recruitment in one unit of time is constant and equal to λ . Then, $C = EC = E\lambda = \lambda$ and $\text{Var}(C) = \text{Var}(\lambda) = 0$, as we can see in Table 3.1.

3.1.2 Expected accrual at time point t

Assuming that recruitments in each unit of time are independent of each other we have:

$$C(t) = E(\underbrace{C + \dots + C}_{t \text{ times}}) = E(\lambda t) = \lambda t$$

$$\text{Var}(C(t)) = \text{Var}(\underbrace{C + \dots + C}_{t \text{ times}}) = t\text{Var}(\lambda) = 0$$

Both the expected accrual and its zero-variance are recorded in Table 3.2 and visualized in Figure 3.1 and Figure 3.4.

3.1.3 Criticism

This is a simple deterministic method based on a linear extrapolation of the constant expected recruitment also called "First Order Recruitment Model" (FORM) (Comfort, 2013). It is also referred to as the *unconditional approach* and its main limitation is the lack of a mechanism to account for known sources of variation in the rate (Carter *et al.*, 2005).

The model based on expectations is overly simplistic and fails to account for changes in center recruitment or the regulatory environment (Barnard *et al.*, 2010). Therefore, stochastic models that incorporate randomness in the recruitment process are more suitable than the widely used deterministic approach (Zhang and Long, 2012).

Methods	Counts	Expectation	Variance	Aleatory	Epistemic
Expectation	$C = \lambda$	λ	0	No	No
Poisson	$C \sim \text{Po}(\lambda)$	λ	λ	Yes	No
Poisson-Gamma	$C \sim \text{Po}(\Lambda); \Lambda \sim \text{G}(\alpha, \beta)$	$\frac{\alpha}{\beta}$	$\frac{\alpha(\beta+1)}{\beta^2}$	Yes	Yes

Table 3.1: Moments and aleatory and epistemic uncertainty of recruitment in one unit of time recruitment covered by different models for counts.

Methods	Counts	Expectation	Variance	Aleatory	Epistemic
Expectation	$C(t) = \lambda t$	λt	0	No	No
Poisson	$C(t) \sim \text{Po}(\lambda t)$	λt	λt	Yes	No
Poisson-Gamma	$C(t) \sim \text{Po}(\Lambda t); \Lambda \sim \text{G}(\alpha, \beta)$	$t \frac{\alpha}{\beta}$	$t \frac{\alpha(\beta+t)}{\beta^2}$	Yes	Yes

Table 3.2: Moments and aleatory and epistemic uncertainty in accrual until t covered by different models for counts.

3.2 Counts: Model based on Poisson Process

One way to incorporate variation in the mean number of participants per day is by assuming that participants are recruited according to a known probability distribution, such as the Poisson distribution (Carter, 2004). This approach emulates trial accrual using a random number generator and records the time required to reach the target sample size over multiple iterations (Carter *et al.*, 2005).

The resulting distribution helps estimate the probability of completing accrual within a given time frame and assess variability in accrual time. This method is particularly useful when a trial has a fixed duration, as it allows researchers to determine the necessary number of clinical centers and monthly recruitment rate to achieve a high probability (e.g., 80%) of completing enrollment on time (Carter *et al.*, 2005).

The Poisson distribution $C \sim \text{Po}(\lambda)$ allows us to explain the recruitment of patients. It is a discrete variable that expresses the probability of a given number of events (in our case, patient recruitment) occurring in a fixed unit interval of time. We assume that these events occur with a known constant rate λ and are independent of each other.

$$P[C=c] = \frac{\lambda^c}{c!} e^{-\lambda}, \quad c = 0, 1, 2, \dots$$

One important property from the Poisson distribution is that it is infinitely divisible (Held and Bové, 2014). If $X_i \sim \text{Po}(\lambda_i)$ for $i = 1, \dots, n$ are independent, then, $\sum_{i=1}^n X_i \sim \text{Po}\left(\sum_{i=1}^n \lambda_i\right)$.

3.2.1 Recruitment in one unit of time

The recruitment of patients in one unit of time follows $C \sim \text{Po}(\lambda)$ and the expectation and variance are $EC = \lambda$ and $\text{Var}(C) = \lambda$, as we can see in Table 3.1

3.2.2 Accrual at time point t

At time point t , the accrual follows $C \sim \text{Po}(\lambda t)$. Using the infinitely divisible property from the Poisson applicable to independent random variables, $\underbrace{\text{Po}(\lambda) + \dots + \text{Po}(\lambda)}_{t \text{ times}} = \text{Po}(\lambda t)$. We assume that the recruitment of patients in t unit time intervals is independent from another. As we can see in Table 3.2, the expectation and variance are the following:

$$\begin{aligned} EC(t) &= \lambda t \\ \text{Var}(C(t)) &= \lambda t \end{aligned}$$

For example, if we assume $\lambda = 0.591$ per day and $t = 550$, we can show the accrual of 100 different studies in Figure 3.1 and the histogram at $t = 550$ days. The exact distribution at $t = 550$ is provided in Figure 3.2 and the Cumulative Distribution Function (CDF) in Figure 3.3. The uncertainty bands based on the exact quantiles are displayed in Figure 3.4.



Figure 3.1: Poisson-distributed counts with $\lambda = 0.591$ per day and uncertainty range. The black line represents the point estimate of the expected accrual from section 3.1, while the red dashed lines indicate Poisson’s 95% aleatory uncertainty. The histogram illustrates the distribution of observed counts in 100 studies at time $t = 550$ days (Spiegelhalter *et al.*, 2011; Liu *et al.*, 2023).

3.2.3 Criticism

This model was used by Carter (2004) and Carter *et al.* (2005). Although this model accounts for aleatory uncertainty, the recruitment rate is assumed to be constant for the entire period of time. Therefore, an alternative method that accounts for varying recruitment rates over time is necessary.

3.3 Counts: Negative Binomial model derived from Poisson-Gamma model

The basic Poisson model does not account for variations in recruitment rates or uncertainties in rate estimates (Mountain and Sherlock, 2022). To address this Anisimov and Fedorov (2007) propose a random effects model where recruitment follows a homogeneous Poisson process with rates drawn from a gamma distribution, a probabilistic model with Poisson-Gamma mixture distribution. In this approach, rates are treated as random variables with a prior gamma distribution, whose parameters are estimated using current recruitment data. This allows for a posterior distribution of rates to be used for recruitment prediction in an empirical Bayesian

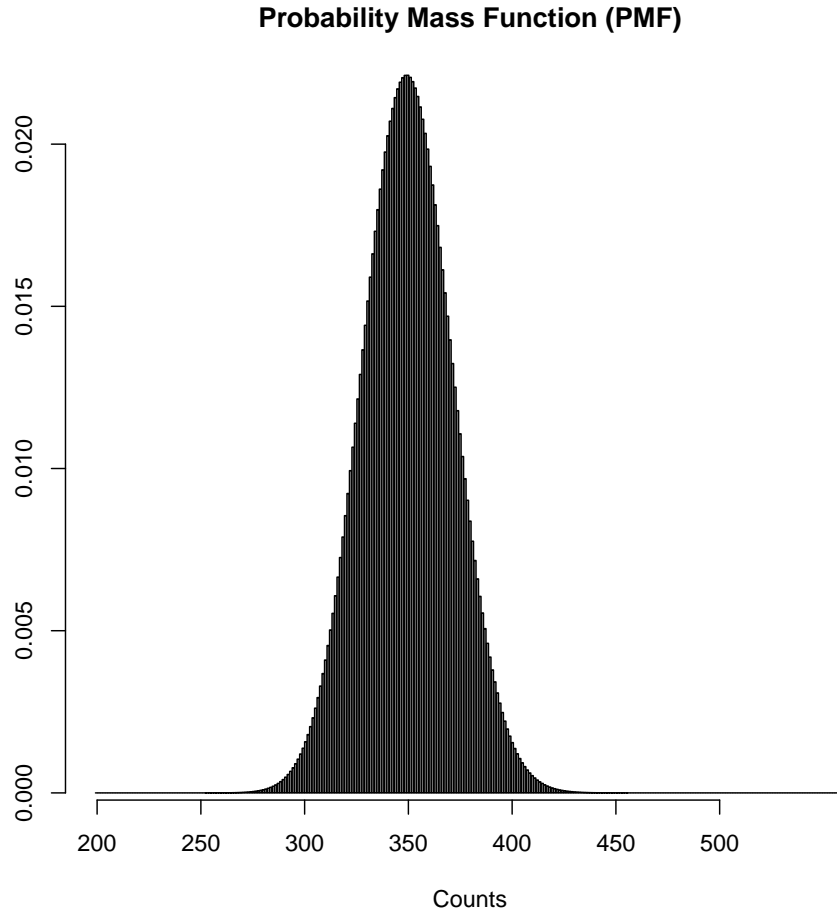


Figure 3.2: Probability Mass Function (PMF) of Poisson-distributed counts: This bar plot represents the probability mass function (PMF) of counts ranging from 200 to 500, using a Poisson distribution $\text{Po}(\lambda t)$ with a rate parameter $\lambda = 0.591$ per day at time $t = 550$ days.

framework.

Building on this, a Poisson-Gamma model can be implemented by randomly generating recruitment rates using a Gamma distribution and plugging them into a Poisson process. This model can be used to make two types of projections: a point prediction estimating when the expected number of events will reach a specific sample size and a Bayesian interval prediction based on the generation of future accrual and event dates. This method enables flexible forecasting for any milestone at any calendar time ([Bagiella and Heitjan, 2001](#)).

3.3.1 Recruitment in one unit of time

Let $C|\Lambda \sim \text{Po}(\Lambda)$ and $\Lambda \sim G(\alpha, \beta)$. Where Λ represents the "recruitment proneness" in the unit of time.

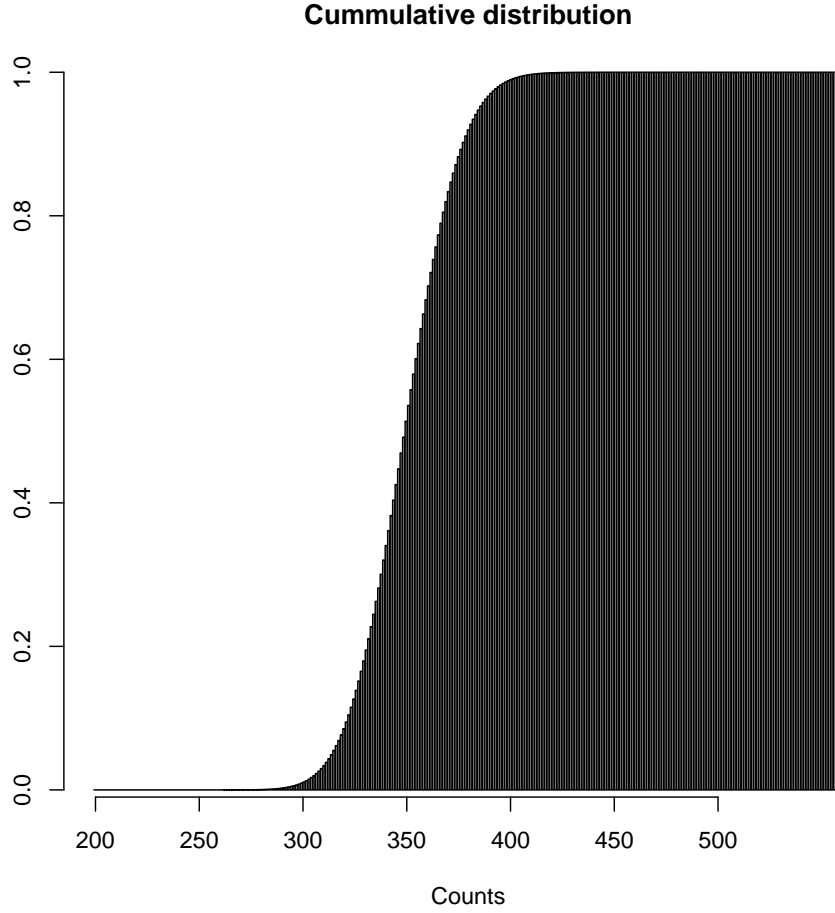


Figure 3.3: Cumulative Distribution Function (CDF) of Poisson-distributed counts: The bar plot illustrates the cumulative probability distribution for counts within the range of 200 to 500, using a Poisson $Po(\lambda t)$ distribution with a rate parameter $\lambda = 0.591$ per day at time $t = 550$ days.

$$\begin{aligned}
 p(c) &= \int_0^\infty p(c|\lambda)p(\lambda)d\lambda \\
 &= \int_0^\infty \frac{\lambda^c \exp(-\lambda)}{c!} \left[\lambda^{\alpha-1} \exp(-\beta\lambda) \frac{\beta^\alpha}{\Gamma(\alpha)} \right] d\lambda \\
 &= \frac{\beta^\alpha}{c! \Gamma(\alpha)} \int_0^\infty \lambda^{\alpha+c-1} \exp(-\lambda) \exp(-\lambda\beta) d\lambda \\
 &= \frac{\beta^\alpha \Gamma(\alpha+c)}{c! \Gamma(\alpha) (\beta+1)^{\alpha+c}} \underbrace{\int_0^\infty \frac{(\beta+1)^{\alpha+c}}{\Gamma(\alpha+c)} \lambda^{\alpha+c-1} \exp(-(\beta+1)\lambda) d\lambda}_{=1} \\
 &= \beta^\alpha \binom{\alpha+c-1}{\alpha-1} \left(\frac{1}{\beta+1} \right)^{\alpha+c} \\
 &= \binom{\alpha+c-1}{\alpha-1} \left(\frac{1}{\beta+1} \right)^c \left(\frac{\beta}{\beta+1} \right)^\alpha \\
 c &= 0, 1, 2, 3, \dots
 \end{aligned}$$

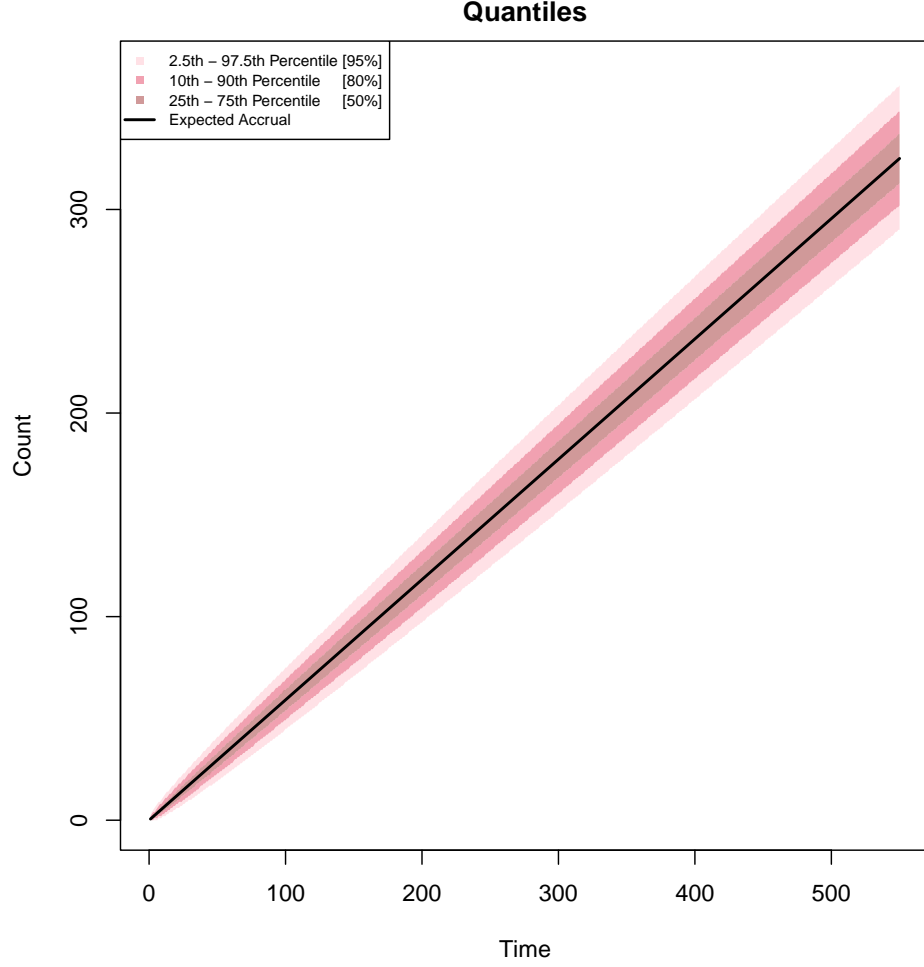


Figure 3.4: Predicted uncertainty bands for Poisson process with $\lambda = 0.591$ per day. The black line represents the expected accrual, while the red shaded regions indicate aleatory uncertainty: the dark red band spans the interquantile range (25th - 75th percentiles), the lighter red band cover the 10th - 90th percentile range and the light red the 2.5th - 97.5th percentile range (Spiegelhalter *et al.*, 2011).

Thus, $C \sim \text{NBin}\left(\alpha, \frac{\beta}{\beta+1}\right)$.

The parameter λ in the integral represents the expected recruitment rate per unit of time for an individual and this recruitment rate is assumed to vary from individual to individual as it is generated by a $G(\alpha, \beta)$ distribution (Johnson *et al.*, 2005).

Using the expressions of iterated expectation and variance (Held and Bové, 2014) and the expectation and variance from the respective random variables $C|\Lambda \sim \text{Po}(\Lambda)$ and $\Lambda \sim G(\alpha, \beta)$, we have that:

$$EC = E_{\Lambda}[E_C(C|\Lambda)] = E_{\Lambda}[\Lambda] = \alpha/\beta$$

$$\begin{aligned} \text{Var}(C) &= \text{Var}_{\Lambda}[E_C(C|\Lambda)] + E_{\Lambda}[\text{Var}_C(C|\Lambda)] \\ &= \text{Var}_{\Lambda}[\Lambda] + E_{\Lambda}[\Lambda] \\ &= \alpha/\beta^2 + \alpha/\beta = \frac{\alpha(\beta + 1)}{\beta^2} \end{aligned}$$

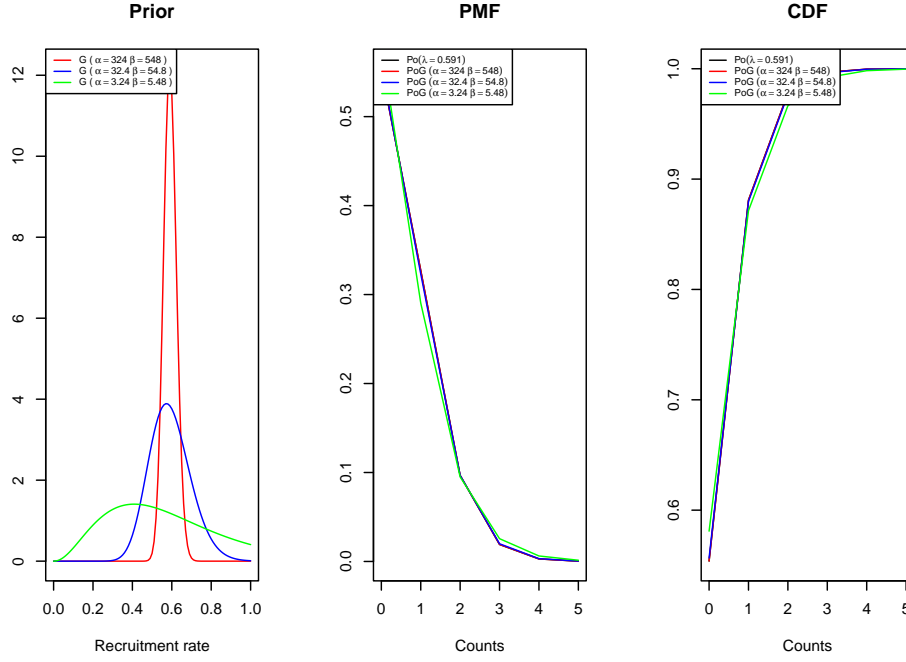


Figure 3.5: Sensitivity analysis between Poisson distribution with $\lambda = 0.591$ and Negative Binomial changing parameters of Gamma prior that maintain same expectation $\frac{\alpha}{\beta} = 0.591$ with $t = 1$.

There are two different interpretations of the Negative Binomial, Failure-Based and Count-based.

3.3.2 Failure-Based

1. The Negative Binomial $X \sim \text{NBin}(r, \pi)$ models the number of **failures** before achieving a fixed number of **successes** in a sequence of Bernoulli trials.
2. Parametrization:
 - n : Number of successes to be achieved (fixed).
 - p : Probability of success in each trial
 - The random variable X represents the number of failures before achieving n successes.
3. Probability Mass Function (PMF) (R Core Team, 2024):

$$P(X=x) = \frac{\Gamma(x+n)}{\Gamma(x)x!} p^n (1-p)^x,$$

$$x = 0, 1, 2, \dots, n > 0$$

$$0 < p \leq 1$$

where x is the number of failures.

4. Interpretation: In a sequence of independent binary trials with constant probability p of observing a *non-recruited* patient, X is the number of *recruited* patients observed at the time that x *non-recruited* patients are observed (Meeker *et al.*, 2017).

With respect to the parameters, $n > 0$ represents the number of successes until the experiment is stopped. The success probability in each experiment is represented by $p \in [0, 1]$. In R the

functions `_nbinom(..., size = n, prob = p)` relate to the random variable $X - r$, the number of successes (as opposed to the number of trials) until r successes have been achieved ([Held and Bové, 2014](#)).

$$EX = \frac{r(1 - \pi)}{\pi}$$

$$Var(X) = \frac{r(1 - \pi)}{\pi^2}$$

Since we will be using the Count-Based interpretation of the Negative Binomial ([Hilbe, 2011](#)), our parametrization relates to R with $n = \alpha$ and $p = \frac{\beta}{\beta+1}$.

3.3.3 Count-Based

1. The Negative Binomial $X \sim \text{NBin}\left(\alpha, \frac{\beta}{\beta+1}\right)$ can also be seen as a Poisson-Gamma mixture, where the observed count data follows a Poisson distribution with a mean that itself follows a Gamma distribution, $C|\Lambda \sim \text{Po}(\Lambda)$ and $\Lambda \sim \text{G}(\alpha, \beta)$.

2. Parametrization:

- $\mu = \frac{\alpha}{\beta}$: Mean of the distribution (expected number of occurrences).
- α : Dispersion parameter, controlling the variance.

3. Alternative formulation of the PMF ([Hilbe, 2011](#)):

$$P(X=c) = \binom{\alpha+c-1}{\alpha-1} \left(\frac{\mu}{\beta+\mu}\right)^c \left(\frac{\alpha}{\alpha+\mu}\right)^\alpha, \quad c \geq 0$$

where c is the counts.

4. Interpretation: This model is used to represent "recruitment proneness". The parameter μ represents the expected number of recruitments in a study ([Johnson *et al.*, 2005](#)).

In the count-based method we take into account the overdispersion of the data. When the variability in the observed data is greater than what is expected.

$$EX = \mu$$

$$\text{Var}X = \mu + \frac{\mu}{\beta}$$

How do we get to our formulation of the PMF:

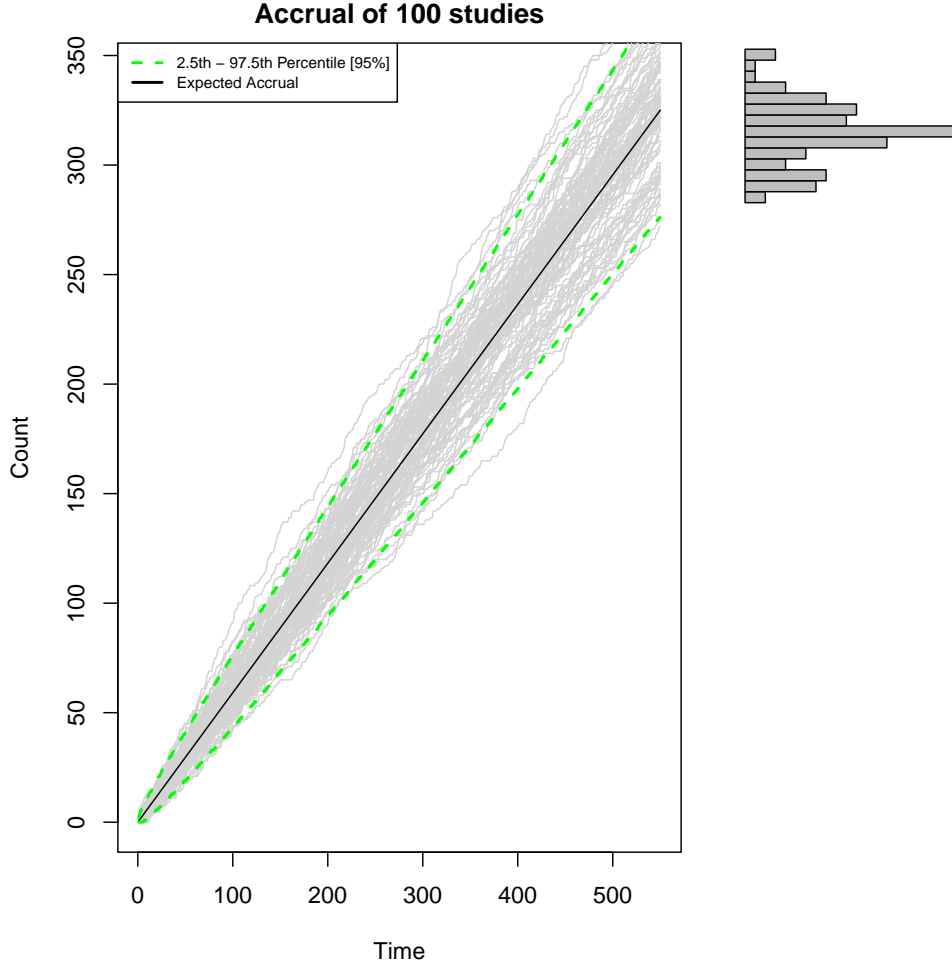


Figure 3.6: Poisson-Gamma ($\alpha = 324, \beta = 548$) distributed counts with $\mu = 0.591$ per day and uncertainty range. The black line represents the point estimate of the expected accrual from Section 3.1, while the red dashed lines indicate Poisson-Gamma 95% aleatory and epistemic uncertainty. The histogram illustrates the distribution of observed counts in 100 studies at time $t = 550$ days (Spiegelhalter *et al.*, 2011; Liu *et al.*, 2023).

$$\begin{aligned}
 P(X = c) &= \binom{\alpha + c - 1}{\alpha - 1} \left(\frac{\mu}{\alpha + \mu} \right)^c \left(\frac{\alpha}{\alpha + \mu} \right)^\alpha \\
 &= \binom{\alpha + c - 1}{\alpha - 1} \left(\frac{\alpha/\beta}{\alpha + \alpha/\beta} \right)^c \left(\frac{\alpha}{\alpha + \alpha/\beta} \right)^\alpha \\
 &= \binom{\alpha + c - 1}{\alpha - 1} \left(\frac{\alpha/\beta}{\alpha\beta/\beta + \alpha/\beta} \right)^c \left(\frac{\alpha}{\alpha\beta/\beta + \alpha/\beta} \right)^\alpha \\
 &= \binom{\alpha + c - 1}{\alpha - 1} \left(\frac{\alpha}{\alpha\beta + \alpha} \right)^c \left(\frac{\beta\alpha}{\alpha\beta + \alpha} \right)^\alpha \\
 &= \binom{\alpha + c - 1}{\alpha - 1} \left(\frac{1}{\beta + 1} \right)^c \left(\frac{\beta}{\beta + 1} \right)^\alpha
 \end{aligned}$$

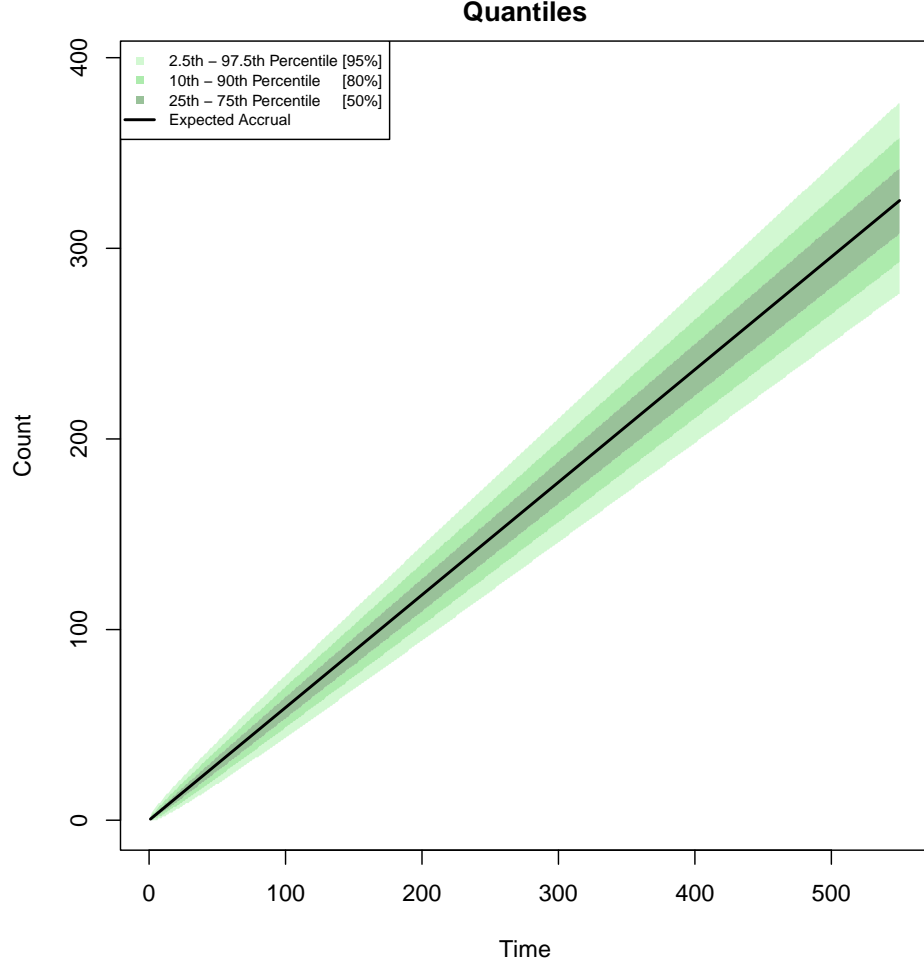


Figure 3.7: Predicted uncertainty bands for Poisson-Gamma process with $\mu = 0.591$ per day. The black line represents the expected accrual, while the green shaded regions indicate aleatory and epistemic uncertainty: the dark green band spans the interquantile range (25th - 75th percentiles), the lighter green band cover the 10th - 90th percentile range and the light green the 2.5th - 97.5th percentile range (Spiegelhalter *et al.*, 2011).

3.3.4 Sensitivity Analysis

In Figures 3.8 and 3.5, the Poisson distribution captures aleatory uncertainty, while the Gamma prior represents epistemic uncertainty. The Poisson-Gamma distribution incorporates both types of uncertainty. The sensitivity analysis, also shown in Figures 3.8 and 3.5, highlights that while the expectation remains unchanged, smaller parameter values lead to greater overall uncertainty due to the increased variance introduced by the Gamma distribution. The smaller the β , the greater the variance.

$$\text{Var}(G(\alpha, \beta)) = \frac{\alpha}{\beta^2} = \frac{E(G(\alpha, \beta))}{\beta}$$

In the Poisson-Gamma model we can interpret α as the parameter that represents the sample size and β represents time.

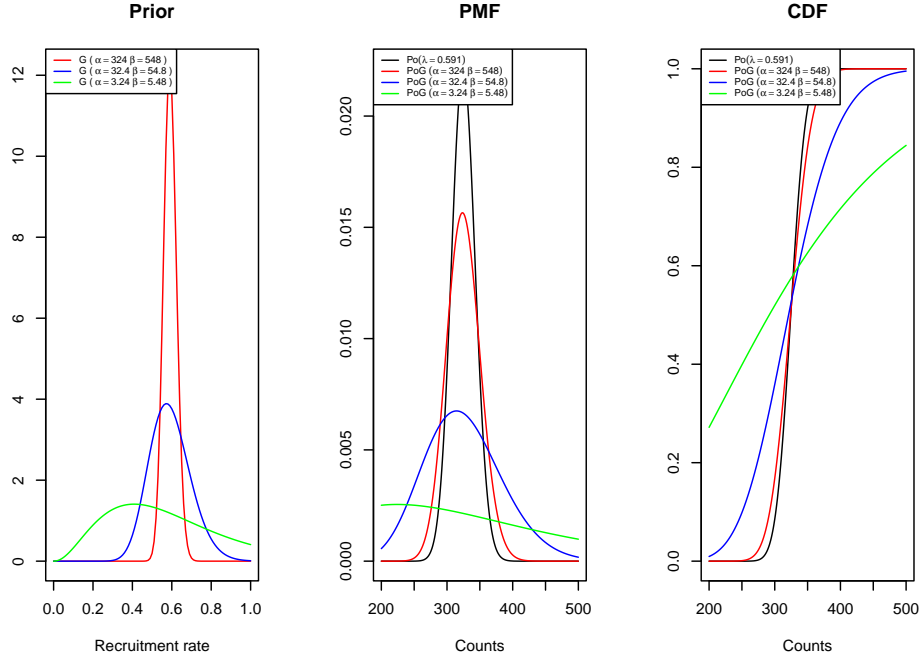


Figure 3.8: Sensitivity analysis between Poisson distribution with $\lambda = 0.591$ and Poisson-Gamma changing parameters of Gamma prior that maintain same expectation $\frac{\alpha}{\beta} = 0.591$ with $t = 550$.

3.3.5 Accrual at time point t

Let $C(t)|\Lambda \sim \text{Po}(\Lambda t)$ and $\Lambda \sim G(\alpha, \beta)$. By the infinitely divisible property of the Poisson distribution we have that $\underbrace{\text{Po}(\Lambda) + \dots + \text{Po}(\Lambda)}_{t \text{ times}} = \text{Po}(\Lambda t)$. This Poisson-Gamma model has parameters t , α and β . Hence, we denote it as $C(t) \sim \text{PoG}(t, \alpha, \beta)$.

$$\begin{aligned}
 p(c) &= \int_0^\infty p(c|\lambda t)p(\lambda)d\lambda \\
 &= \int_0^\infty \frac{(\lambda t)^c \exp(-\lambda t)}{c!} \left[(\lambda)^{\alpha-1} \exp(-\beta\lambda) \frac{\beta^\alpha}{\Gamma(\alpha)} \right] d\lambda \\
 &= \frac{\beta^\alpha t^c}{c! \Gamma(\alpha)} \int_0^\infty \lambda^{\alpha+c-1} \exp(-\lambda t) \exp(-\lambda \beta) d\lambda \\
 &= \frac{\beta^\alpha \Gamma(\alpha+c) t^c}{c! \Gamma(\alpha) (\beta+t)^{\alpha+c}} \underbrace{\int_0^\infty \frac{(\beta+t)^{\alpha+c}}{\Gamma(\alpha+c)} \lambda^{\alpha+c-1} \exp(-(\beta+t)\lambda) d\lambda}_{=1} \\
 &= \beta^\alpha t^c \binom{\alpha+c-1}{\alpha-1} \left(\frac{1}{\beta+t} \right)^{\alpha+c} \\
 &= \binom{\alpha+c-1}{\alpha-1} \left(\frac{t}{\beta+t} \right)^c \left(\frac{\beta}{\beta+t} \right)^\alpha \\
 c &= 0, 1, 2, 3, \dots
 \end{aligned}$$

Thus, $C(t) \sim \text{NBin}\left(\alpha, \frac{\beta}{\beta+t}\right)$

We will be focusing on the count-based interpretation of the Negative Binomial distribution. We can relate this interpretation to the more popular failure-based interpretation by seeing α as n , the number of successes. In our case, the number of patients we wish to recruit. And, $p = \frac{\beta}{\beta+t}$ which is the probability of success, as the probability of recruiting.

Using the expressions of iterated expectation and variance (Held and Bové, 2014) and the expectation and variance from the respective random variables $C(t)|\Lambda \sim \text{Po}(\Lambda t)$ and $\Lambda \sim \text{G}(\alpha, \beta)$, we have that:

$$\text{E}(C(t)) = \text{E}_{\Lambda}[\text{E}_{C(t)}(C(t)|\Lambda)] = \text{E}_{\Lambda}[\Lambda t] = t\alpha/\beta$$

$$\begin{aligned} \text{Var}(C(t)) &= \text{Var}_{\Lambda}[\text{E}_{C(t)}(C(t)|\Lambda)] + \text{E}_{\Lambda}[\text{Var}_{C(t)}(C(t)|\Lambda)] \\ &= \text{Var}_{\Lambda}[\Lambda t] + \text{E}_{\Lambda}[\Lambda t] \\ &= t^2\alpha/\beta^2 + t\alpha/\beta = \frac{t\alpha(\beta+t)}{\beta^2} \end{aligned}$$

Therefore, we clearly have overdispersion $\text{Var}(C(t)) > \text{E}(C(t))$. This can be easily seen because:

$$\begin{aligned} \text{Var}(C(t)) &= \text{E}(C(t)) \frac{\beta+t}{\beta} \\ &= \text{E}(C(t)) \left(1 + \frac{t}{\beta}\right) \end{aligned}$$

3.4 Comparison of models for the accrual of counts

As we can see in Figures 3.9 and 3.11, we are taking into account more epistemic uncertainty of the recruitment rate Λ in the Poisson-Gamma model than we do in the Poisson process where λ is fixed. Hence, the color-coding, red for only aleatory and green, aleatory and epistemic. In reality we expect fluctuations of recruitment rates, therefore, the Poisson-Gamma model is more realistic.

Figures 3.9 and 3.11 assume that the recruitment rates do not vary much by assuming $\text{G}(\alpha = 324, \beta = 548)$ as prior, where the expectation is 0.591 and the standard deviation 0.033. In contrast, Figures 3.10 and 3.12, assume a less informative prior $\text{G}(\alpha = 32.4, \beta = 54.8)$ of the recruitment rates with expectation 0.591 and empirical standard deviation 0.104, showing a more pronounced discrepancy between the Poisson and the Poisson-Gamma process.

3.5 Generation of Poisson-Gamma model

There are two ways with which we can generate the random Λ in the $\text{PoG}(t, \alpha, \beta)$ model and we will investigate in this section whether they are both equivalent.

3.5.1 Version 1

We generate a random vector of λ values of length $M = 10^5$ with $\text{G}(\alpha, \beta)$ and a vector of counts at each time point, of length t with $\text{Po}(\lambda)$. For the final counts we sum cumulatively (cumsum) the counts at t so that we get the accrual of patients at time t of each study.

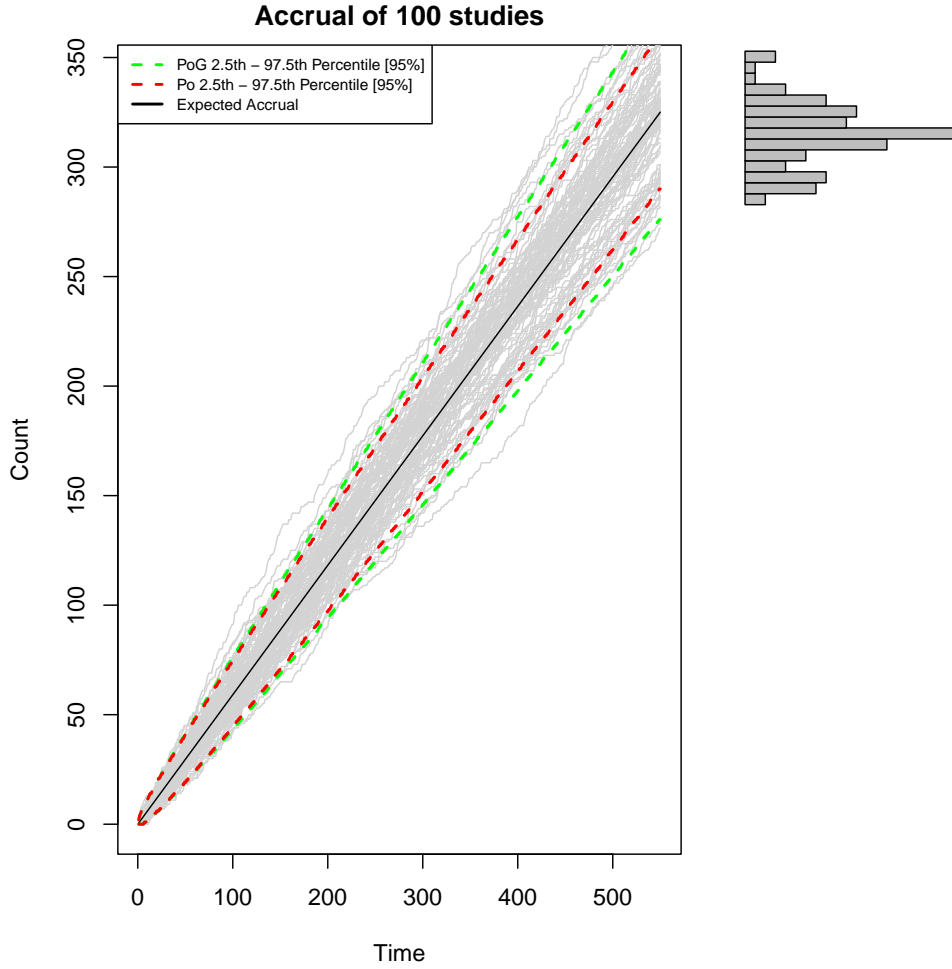


Figure 3.9: Comparison of the 95% uncertainty range taken into consideration in the Poisson-Gamma ($\alpha = 324, \beta = 548$) model as opposed to the Poisson $\lambda = 0.591$ (Spiegelhalter *et al.*, 2011; Liu *et al.*, 2023).

$$\begin{aligned} \lambda^m &\sim G(\alpha, \beta) \\ C(t)^m &\sim \text{Po}(\lambda^m t) = \underbrace{\text{Po}(\lambda^m) + \dots + \text{Po}(\lambda^m)}_{t \text{ times}} \\ m &= 1, \dots, M \end{aligned}$$

```
set.seed(2025)

M <- 10^4
t <- seq(1, 550, 1)
lambda <- 0.591
alpha <- 32.4
beta <- 54.8

cval_cum_matrix <- matrix(NA, nrow = M, ncol = length(t))
v_lambda <- rgamma(M, shape = alpha, rate = beta)
```

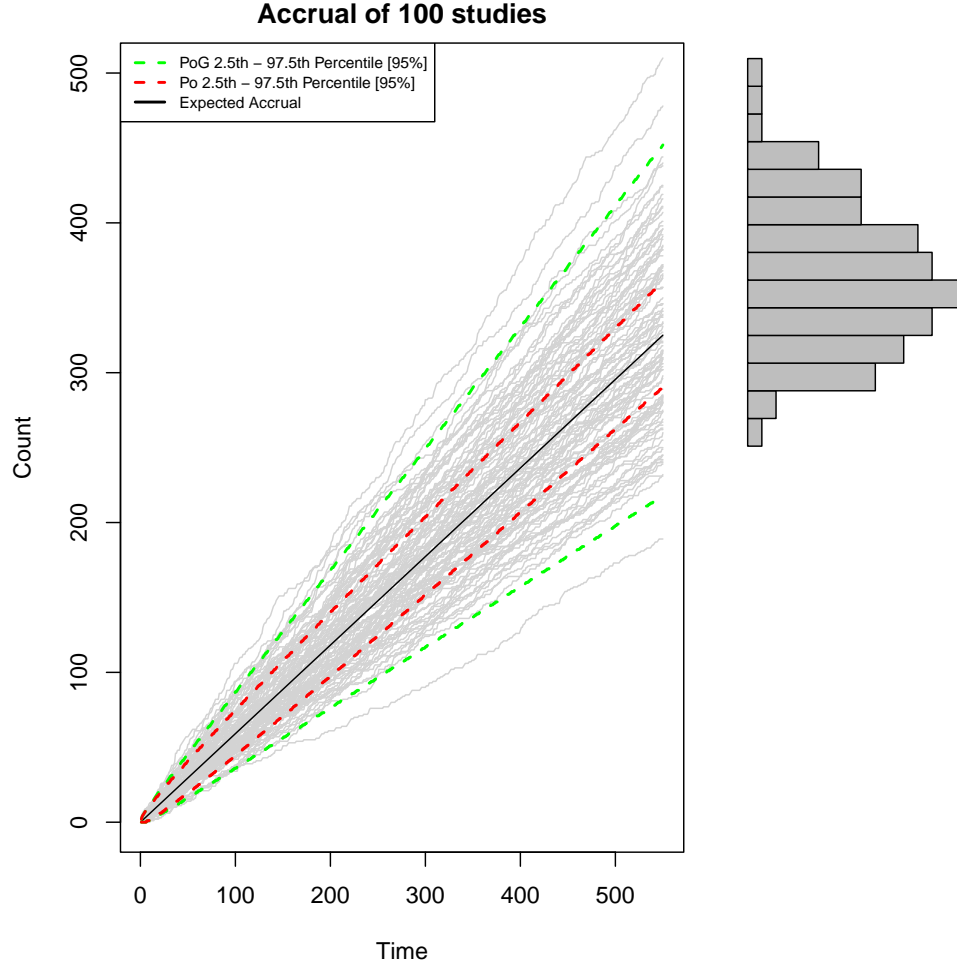


Figure 3.10: Comparison of the 95% uncertainty range taken into consideration in the Poisson-Gamma ($\alpha = 32.4, \beta = 54.8$) model as opposed to the Poisson $\lambda = 0.591$ (Spiegelhalter *et al.*, 2011; Liu *et al.*, 2023).

```
for (i in 1:M) {
  cval <- rpois(length(t), lambda = v_lambda[i])
  cval_cum_matrix[i, ] <- cumsum(cval)
}
```

3.5.2 Version 2

At each time point $i = 1, \dots, t$, we generate a $\lambda^{(i)}$ with $G(\alpha, \beta)$ and a count with $Po(\lambda^{(i)})$. For the final counts we sum cumulatively (cumsum) the counts at t so that we get the accrual of patients at time t of each study.

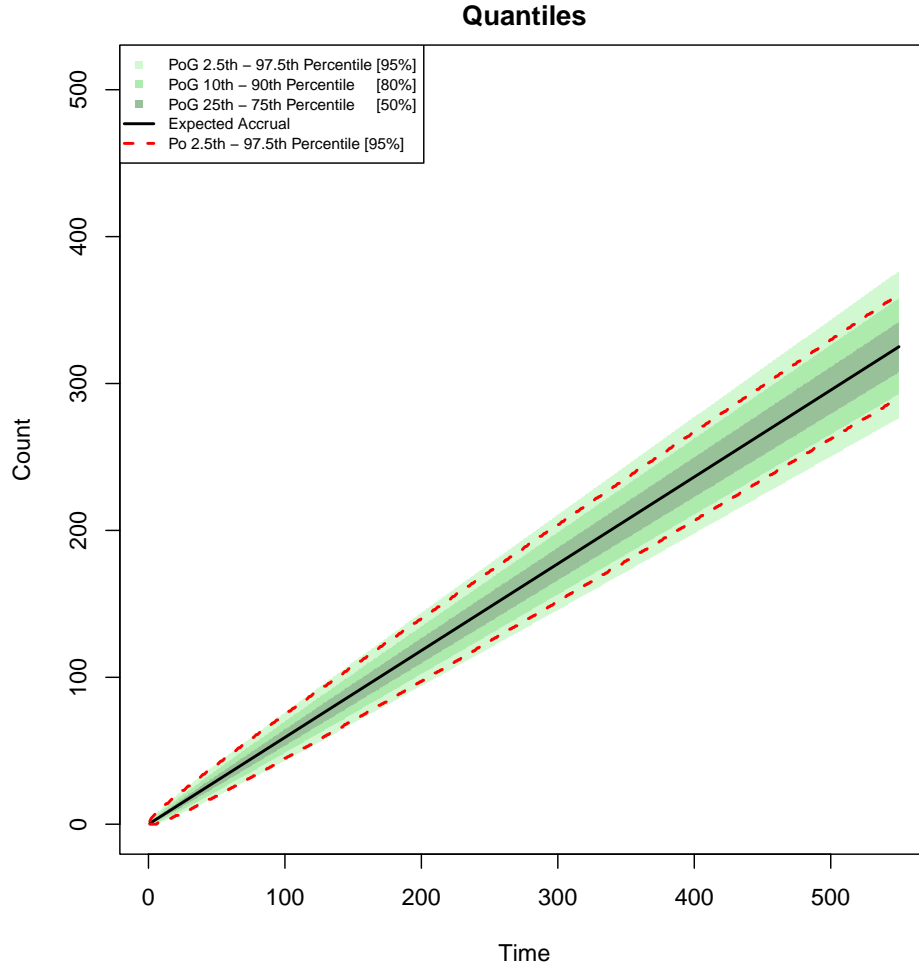


Figure 3.11: Comparison of the theoretical quantiles in the Poisson-Gamma ($\alpha = 324, \beta = 548$) model and the 95% uncertainty range of the Poisson $\lambda = 0.591$ (Spiegelhalter *et al.*, 2011; Liu *et al.*, 2023).

$$\begin{aligned}\lambda^{(i)m} &\sim G(\alpha, \beta) \\ C(i)^m &\sim \text{Po}(\lambda^{(i)m}) \\ C(t)^m &= \sum_{i=1}^t C(i)^m \\ i &= 1, \dots, t \\ m &= 1, \dots, M\end{aligned}$$

```
set.seed(2025)

M <- 10^4
t <- seq(1, 550, 1)
lambda <- 0.591
alpha <- 32.4
beta <- 54.8
```

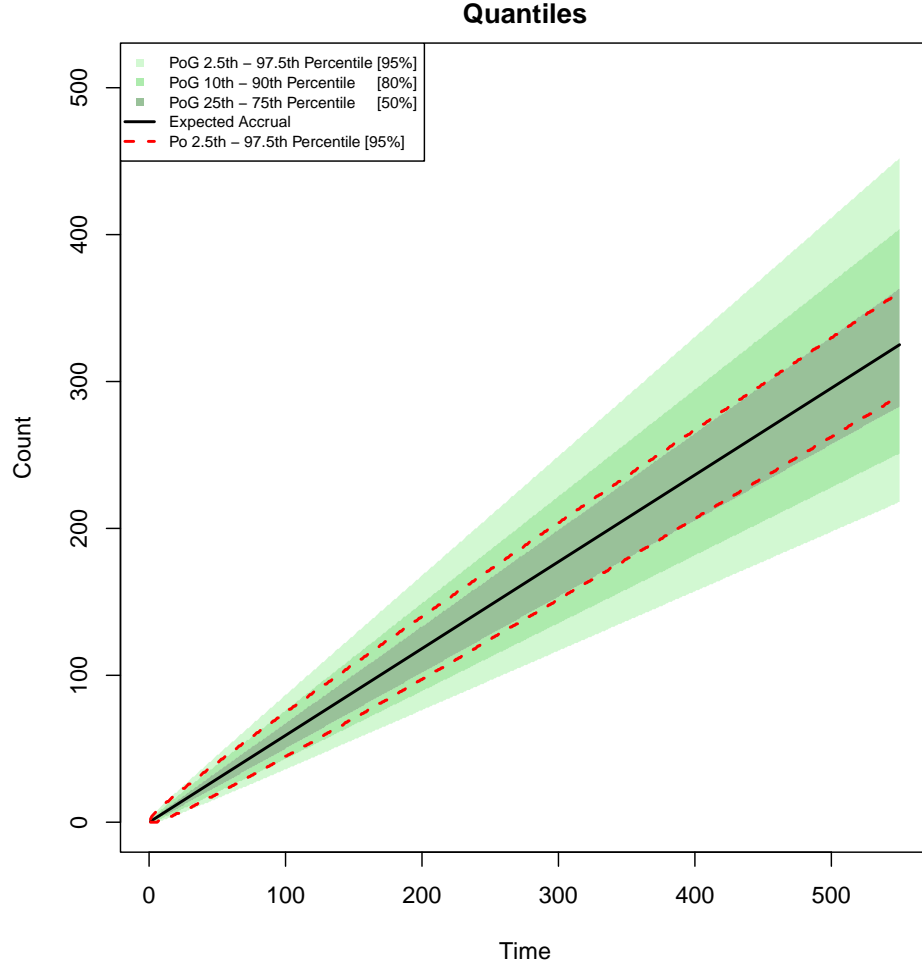


Figure 3.12: Comparison of the theoretical quantiles in the Poisson-Gamma ($\alpha = 32.4, \beta = 54.8$) model and the 95% uncertainty range of the Poisson $\lambda = 0.591$ (Spiegelhalter *et al.*, 2011; Liu *et al.*, 2023).

```
cval_cum_matrix_2 <- matrix(NA, nrow = M, ncol = length(t))
cval <- rep(NA, length(t))

for (i in 1:M) {
  for(j in 1:length(t)){
    cval[j] <- rpois(1, lambda = rgamma(1, shape = alpha, rate = beta))
  }
  cval_cum_matrix_2[i, ] <- cumsum(cval)
}
```

As we can see in Figure 3.13, the density of these two versions do not overlap and therefore we can empirically conclude that these two ways of simulating the Poisson-Gamma model are not equivalent. Both methods share the same expectation but the spread differs. We can see these both in Figure 3.13 and theoretically. In Version 1, we have a $C(t)|\Lambda \sim \text{Po}(\Lambda t)$ with $\Lambda \sim G(\alpha, \beta)$ with expectation and variance (proved above):

$$E(C(t)) = \frac{t\alpha}{\beta}$$

$$\text{Var}(C(t)) = \frac{t\alpha(\beta + t)}{\beta^2}$$

Whereas in Version 2, we have a $C(t)|\Lambda^* \sim \text{Po}(\Lambda^*)$ with $\Lambda^* \sim G(t\alpha, \beta)$ because:

$$\begin{aligned} \sum_{i=1}^t C_i &= \sum_{i=1}^t \text{Po}(\lambda_i) \\ &= \text{Po}\left(\sum_{i=1}^t \lambda_i\right) \\ &= \text{Po}\left(\sum_{i=1}^t G(\alpha, \beta)\right) \\ &= \text{Po}(G(t\alpha, \beta)) \end{aligned}$$

with,

$$E(C(t)) = \frac{t\alpha}{\beta}$$

and using the variance iterated formula ([Held and Bové, 2014](#)),

$$\begin{aligned} \text{Var}(C(t)) &= \text{Var}_{\Lambda}[E_{C(t)}(C(t)|\Lambda^*)] + E_{\Lambda^*}[\text{Var}_{C(t)}(C(t)|\Lambda^*)] \\ &= \frac{t\alpha}{\beta} + \frac{t\alpha}{\beta^2} \\ &= \frac{t\alpha(\beta + 1)}{\beta^2} \end{aligned}$$

Hence, the spread in Version 2 is smaller than in Version 1. Version 1 for Counts and Time will be used in Chapter 5.

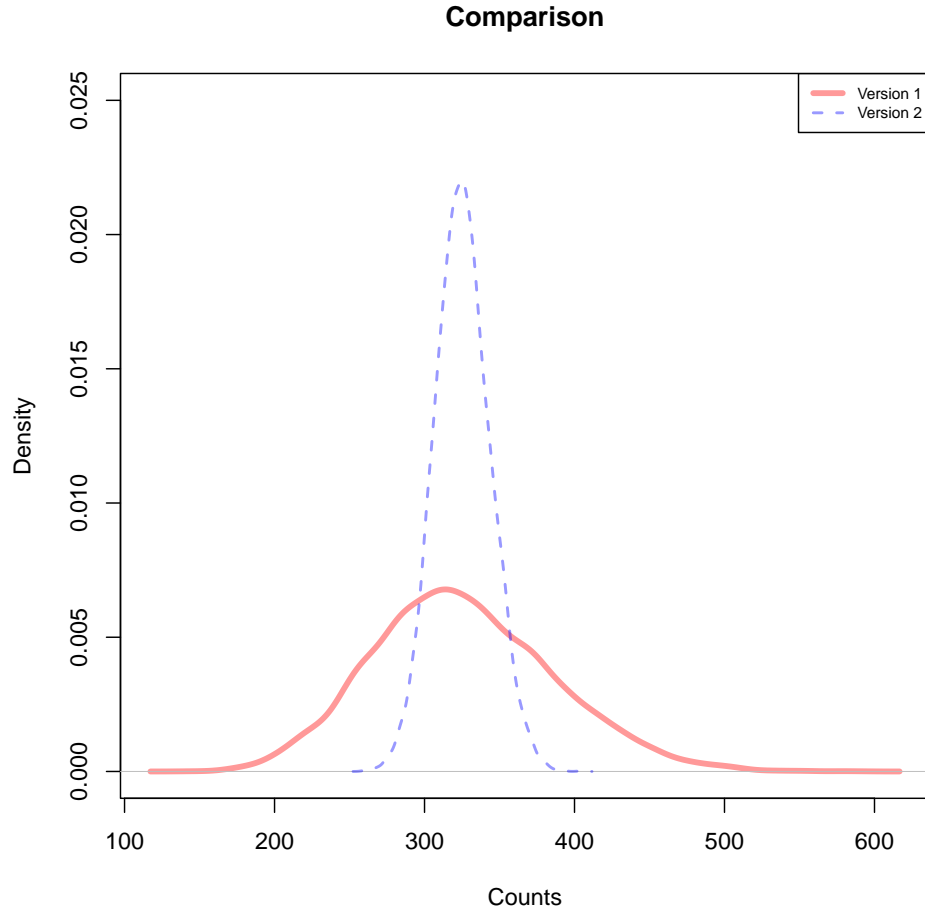


Figure 3.13: Comparison of the two versions with which we can generate a Poisson-Gamma model. Version 1: generates for each $m = 1, \dots, M$, a vector of λ with length $M = 10^4$ using a $G(\alpha = 32.4, \beta = 54.8)$ and then uses each of these random λ^m s to generate t independent $\text{Po}(\lambda^m)$ counts. Version 2: at each time point a different random λ is generated from $G(\alpha = 32.4, \beta = 54.8)$. We compare both these versions at accrual of time $t = 550$ for $\lambda = 0.591$.

Chapter 4

Methods for Waiting Time

4.1 Time: Model based on Expectations

If we fix the sample size of a study at c and we expect the recruitment rate to be λ , we deterministically predict the time planned for the study (without taking into consideration any uncertainty) to be $\hat{T} = \frac{c}{\lambda}$ (Bagiella and Heitjan, 2001). Researchers tend to use simple unconditional methods (White and Hind, 2015). Regarding the expectation and variance in this framework: $ET = E(c/\lambda) = c/\lambda$ and $\text{Var}(T) = \text{Var}(c/\lambda) = 0$, as we can see in Table 4.1.

Methods	Time	Expectation	Variance	Aleatory	Epistemic
Expectation	$T(c) = c/\lambda$	c/λ	0	No	No
Erlang	$T(c) \sim G(c, \lambda)$	c/λ	c/λ^2	Yes	No
Gamma-Gamma	$T(c) \sim G(c, \Lambda); \Lambda \sim G(\alpha, \beta)$	$c \frac{\beta}{\alpha-1}$	$\frac{c\beta^2(c+\alpha-1)}{(\alpha-1)^2(\alpha-2)}$	Yes	Yes

Table 4.1: Moments and aleatory and epistemic uncertainty of recruitment covered by different models for time having a fixed sample size c .

4.2 Time: Model based on Erlang distribution

Let $T(c)$ denote the waiting time until c objects are recruited. For a fixed sample size c , assuming we have a fixed recruitment rate λ , $T(c) \sim G(c, \lambda)$. Since c is an integer, we can use the additivity property from the Gamma distribution applicable to independent random variables, $\underbrace{\text{Exp}(\lambda) + \dots + \text{Exp}(\lambda)}_{c \text{ times}} = G(c, \lambda)$. Moreover, this distribution is also called the Erlang distribution and can be denoted as $\text{Erlang}(c, \lambda)$. As we can see in Table 4.1, the expectation and variance are the following:

$$\begin{aligned} ET(c) &= c/\lambda \\ \text{Var}(T(c)) &= c/\lambda^2 \end{aligned}$$

The Erlang model explains only the aleatory uncertainty of the waiting time until c objects have been recruited. We can visualize the waiting time in Figure 4.3.

4.3 Time: Derivation of Gamma-Gamma model

To take into account the epistemic uncertainty of recruitment rates and the aleatory uncertainty of waiting times, a Gamma-Gamma model is recommended (Bagiella and Heitjan, 2001),

$T(c)|\Lambda \sim G(c, \Lambda)$ and $\Lambda \sim G(\alpha, \beta)$. This Gamma-Gamma model has parameters c , α and β . Thus, $T(c) \sim GG(c, \alpha, \beta)$.

$$\begin{aligned}
p(t) &= \int_0^\infty p(t|\lambda)p(\lambda)d\lambda \\
&= \int_0^\infty \left(\frac{\lambda^c t^{c-1} \exp(-\lambda t)}{\Gamma(c)} \right) \left(\frac{\beta^\alpha \lambda^{\alpha-1} \exp(-\beta \lambda)}{\Gamma(\alpha)} \right) d\lambda \\
&= \frac{t^{c-1} \beta^\alpha}{\Gamma(c)\Gamma(\alpha)} \int_0^\infty \lambda^{c+\alpha-1} \exp(-\lambda(\beta+t)) d\lambda \\
&= \frac{\Gamma(\alpha+c)}{\Gamma(c)\Gamma(\alpha)} \frac{t^{c-1} \beta^\alpha}{(\beta+t)^{\alpha+c}} \underbrace{\int_0^\infty \frac{(\beta+t)^{\alpha+c}}{\Gamma(\alpha+c)} \lambda^{c+\alpha-1} \exp(-\lambda(\beta+t)) d\lambda}_{=1} \\
&= \frac{\Gamma(\alpha+c)}{\Gamma(c)\Gamma(\alpha)} \frac{t^{c-1} \beta^\alpha}{(\beta+t)^{\alpha+c}} \\
&= \frac{\beta^\alpha}{\mathbf{B}(\alpha, c)} \frac{t^{c-1}}{(\beta+t)^{\alpha+c}}
\end{aligned}$$

Thus, $T(c) \sim GG(c, \alpha, \beta)$, see [Held and Bové \(2014\)](#), where they use a slightly different notation.

Using the expressions of iterated expectation and variance ([Held and Bové, 2014](#)), the expectation and variance from the respective random variables $T(c)|\Lambda \sim G(c, \Lambda)$ and $\Lambda \sim G(\alpha, \beta)$, and the fact that when $\Lambda \sim G(\alpha, \beta)$ then, $\frac{1}{\Lambda} \sim \text{IG}(\alpha, \beta)$ with:

$$\begin{aligned}
\mathbb{E} \left[\frac{1}{\Lambda} \right] &= \mathbb{E}(\text{IG}(\alpha, \beta)) = \frac{\beta}{\alpha - 1} \\
\text{Var} \left[\frac{1}{\Lambda} \right] &= \text{Var}(\text{IG}(\alpha, \beta)) = \frac{\beta^2}{(\alpha - 1)^2(\alpha - 2)}
\end{aligned}$$

We have that:

$$\mathbb{E}T(c) = \mathbb{E}_\Lambda[\mathbb{E}_{T(c)}(T(c)|\Lambda)] = \mathbb{E}_\Lambda \left[\frac{c}{\Lambda} \right] = c\mathbb{E}_\Lambda \left[\frac{1}{\Lambda} \right] = c \frac{\beta}{\alpha - 1}, \quad \alpha > 1$$

$$\begin{aligned}
\text{Var}(T(c)) &= \text{Var}_\Lambda[\mathbb{E}_{T(c)}(T(c)|\Lambda)] + \mathbb{E}_\Lambda[\text{Var}_{T(c)}(T(c)|\Lambda)] \\
&= \text{Var}_\Lambda \left[\frac{c}{\Lambda} \right] + \mathbb{E}_\Lambda \left[\frac{c}{\Lambda^2} \right] \\
&= c^2 \text{Var}_\Lambda \left[\frac{1}{\Lambda} \right] + c\mathbb{E}_\Lambda \left[\frac{1}{\Lambda^2} \right] \\
&= \frac{c^2 \beta^2}{(\alpha - 1)^2(\alpha - 2)} + \frac{c\beta^2}{(\alpha - 1)(\alpha - 2)} \\
&= \frac{c\beta^2(c + \alpha - 1)}{(\alpha - 1)^2(\alpha - 2)}, \quad \alpha > 2
\end{aligned}$$

As we can see in Table 4.1. Here, we have again, a clear example of overdispersion because the variance is larger than the expectation:

$$\begin{aligned}\text{Var}(T(c)) &= E(T(c)) \frac{\beta(c + \alpha - 1)}{(\alpha - 1)(\alpha - 2)} \\ &= E(T(c)) \beta \left(\frac{c}{(\alpha - 1)(\alpha - 2)} + \frac{1}{\alpha - 2} \right)\end{aligned}$$

For small parameter α ($\alpha > 2$) and large parameter β , we will have larger uncertainty (variance).

To compute $E_{\Lambda} \left[\frac{1}{\Lambda^2} \right]$ we use property $\text{Var}X = EX^2 - (EX)^2$, therefore, $EX^2 = \text{Var}X + (EX)^2$.

Thus,

$$\begin{aligned}E_{\Lambda} \left[\frac{1}{\Lambda^2} \right] &= \text{Var} \left[\frac{1}{\Lambda} \right] + \left[E \frac{1}{\Lambda} \right]^2 \\ &= \frac{\beta^2}{(\alpha - 1)^2(\alpha - 2)} + \frac{\beta^2}{(\alpha - 1)^2} \\ &= \frac{\beta^2(1 + \alpha - 2)}{(\alpha - 1)^2(\alpha - 2)} \\ &= \frac{\beta^2}{(\alpha - 1)(\alpha - 2)}\end{aligned}$$

For Version 2 of generating Λ^* with $T(c)|\Lambda^* \sim G(c, \Lambda^*)$ and $\Lambda^* \sim G(t\alpha, \beta)$, we have as expectation and variance:

$$ET(c) = E_{\Lambda^*}[E_{T(c)}(T(c)|\Lambda^*)] = E_{\Lambda^*} \left[\frac{c}{\Lambda^*} \right] = cE_{\Lambda^*} \left[\frac{1}{\Lambda^*} \right] = c \frac{\beta}{t\alpha - 1}, \quad t\alpha > 1$$

$$\begin{aligned}\text{Var}(T(c)) &= \text{Var}_{\Lambda^*}[E_{T(c)}(T(c)|\Lambda^*)] + E_{\Lambda^*}[\text{Var}_{T(c)}(T(c)|\Lambda^*)] \\ &= \text{Var}_{\Lambda^*} \left[\frac{c}{\Lambda^*} \right] + E_{\Lambda^*} \left[\frac{c}{\Lambda^{*2}} \right] \\ &= c^2 \text{Var}_{\Lambda^*} \left[\frac{1}{\Lambda^*} \right] + cE_{\Lambda^*} \left[\frac{1}{\Lambda^{*2}} \right] \\ &= \frac{c^2\beta^2}{(t\alpha - 1)^2(t\alpha - 2)} + \frac{c\beta^2}{(t\alpha - 1)(t\alpha - 2)} \\ &= \frac{c\beta^2(c + t\alpha - 1)}{(t\alpha - 1)^2(t\alpha - 2)}, \quad t\alpha > 2\end{aligned}$$

For $t > 1$ this variance from Version 2 is smaller than $\frac{c\beta^2(c+\alpha-1)}{(\alpha-1)^2(\alpha-2)}$, when accrual follows Version 1. We get a narrower distribution if Version 2 is applicable. In Chapter 5, we consider only Version 1 with a higher spread as [Carter \(2004\)](#) suggested (constant λ over time).

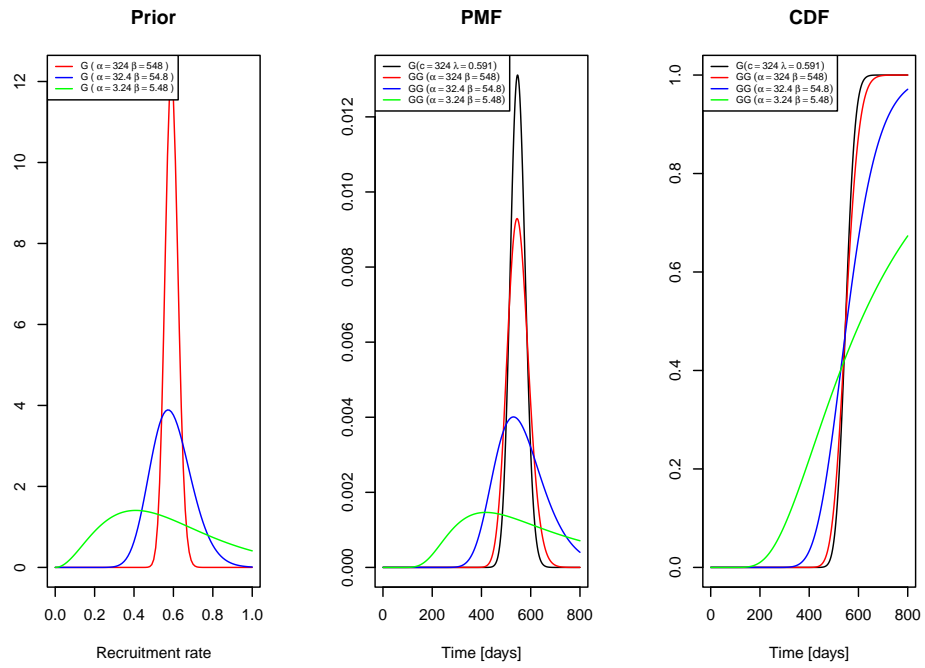


Figure 4.1: Sensitivity analysis between Erlang distribution with $c = 324$ and $\lambda = 0.591$ and Gamma-Gamma model at $c = 324$ changing the parameters of Gamma prior that maintain same expectation $\frac{\alpha}{\beta} = 0.591$, $GG(c = 324, \alpha, \beta)$.

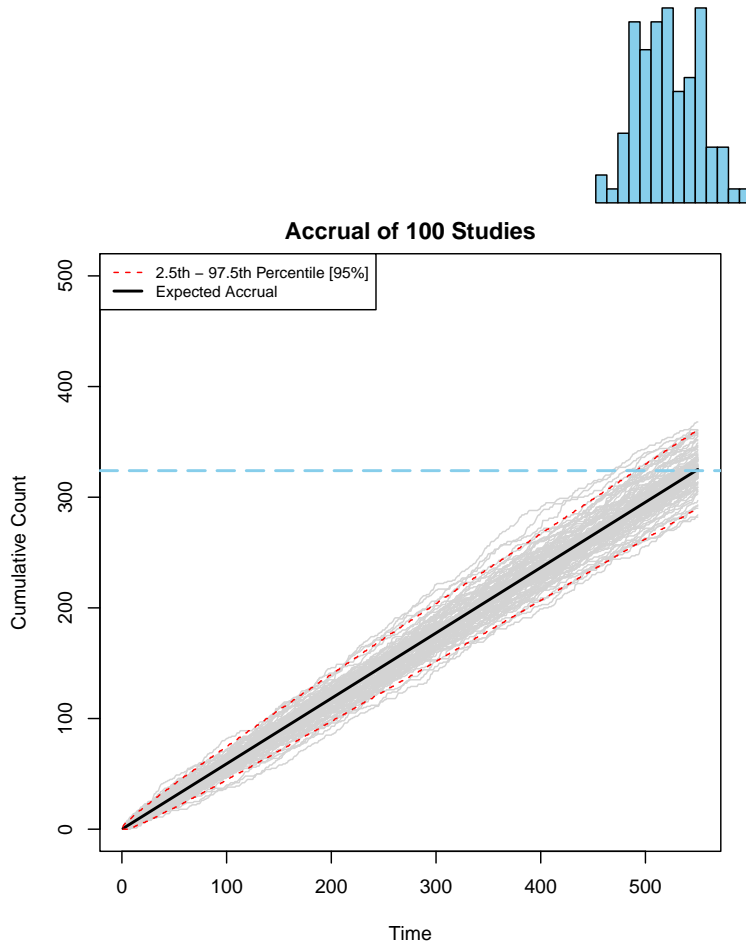


Figure 4.2: Poisson-distributed counts with $\lambda = 0.591$ per day and uncertainty range. The black line represents the point estimate of the expected accrual from Section 3.1, while the red dashed lines indicate Poisson’s 95% aleatory uncertainty. The histogram on the top illustrates the distribution of waiting times to accrue $c = 324$ objects when the recruitment rate per unit of time is $\lambda = 0.591$, modelling waiting time with $T(c) \sim \text{Erlang}(c = 324, \lambda = 0.591)$ (Spiegelhalter *et al.*, 2011; Liu *et al.*, 2023).

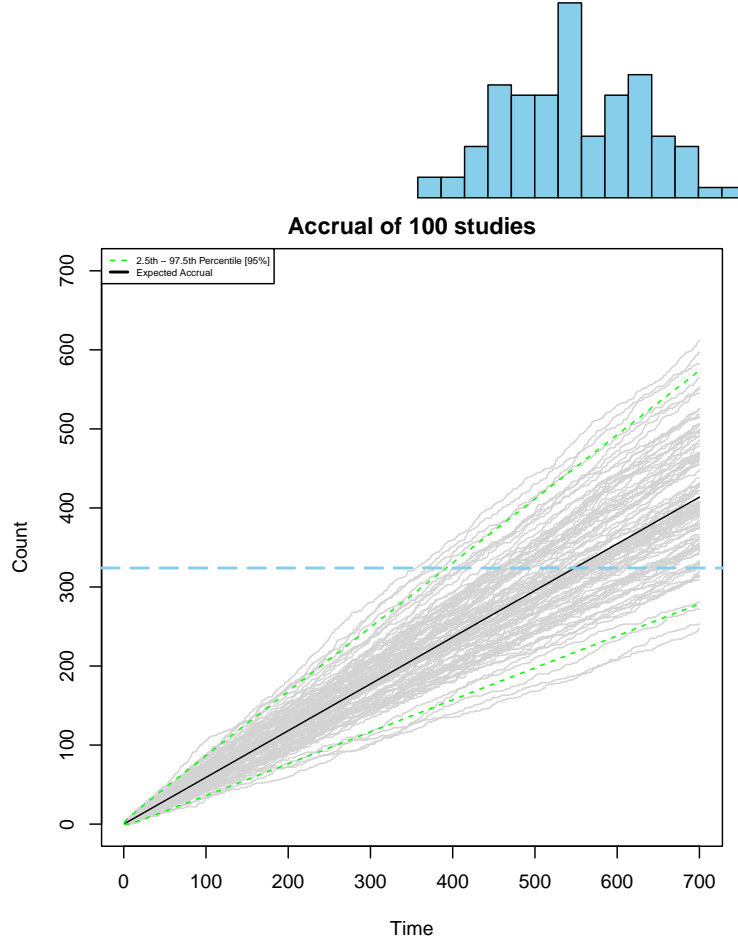


Figure 4.3: Poisson-Gamma ($\alpha = 32.4, \beta = 54.8$) distributed counts with $\lambda = 0.591$ per day and uncertainty range. The black line represents the point estimate of the expected accrual from Section 3.1, while the green dashed lines indicate Poisson-Gamma 95% aleatory and epistemic uncertainty. The histogram on the top illustrates the distribution of waiting times to accrue $c = 324$ objects when the recruitment rate per unit of time follows $\Lambda \sim G(\alpha = 32.4, \beta = 54.8)$, modelling waiting time with $T(c) \sim GG(c = 324, \alpha = 32.4, \beta = 54.8)$ (Spiegelhalter *et al.*, 2011; Liu *et al.*, 2023).

Chapter 5

Results

5.1 Example from Carter

The clinical trial aims to assess the palliative effects of radiation therapy and esophageal stents in terminal esophageal cancer patients. It plans to enroll $C_{target} = 324$ participants, with an expected accrual rate of 18 subjects per month (or about 0.591 per day) across multiple centers. A simple estimate suggests that recruitment will take 18 months or $T_{target} = 548$ days ($324/18$), assuming a constant enrollment rate. However, the proposed method in the study evaluates whether this estimate is realistic and feasible using Monte Carlo (MC) simulations (Carter, 2004).

Before running simulations, it's assumed that participant arrivals follow a Poisson process with a constant rate over 18 months (548 days). This results in a Poisson distribution with a mean of $\lambda = 0.591 \cdot 548 = 324$ participants, matching the trial's target. This approach allows assigning probabilities to different recruitment durations, helping assess how likely it is to meet the enrollment goal within the planned timeframe.

5.2 Pros and cons of Monte Carlo simulations

Carter suggests using Monte Carlo simulations, independent and identically distributed realizations of random variables. One clear advantage of MC simulations is their flexibility, as we can simulate any distribution we want. However, we must consider the following when we use MC simulations instead of the exact probability distribution:

- M , the number of simulations
- Set a seed for computational reproducibility
- Monte Carlo standard errors (MCse) of estimates based on MC simulations
- Pseudo random numbers generated in R rely in the assumption that these pseudo random numbers are close to the true realizations of random variables (Held and Bové, 2014)

5.3 Important questions when forecasting recruitment at the design-stage of a study

By normal approximation to the Poisson distribution $C(t) \sim N(\mu = \lambda t, \sigma^2 = (\lambda t)^2)$, we know that the probability of recruiting the desired N participants is 0.5. Which means that the study has 50% chance of obtaining the desired sample size in the suggested T (Carter, 2004). We would also be assuming that the recruitment rate is constant over time.

In fact, we do not need normal approximation to see this. This can be shown with the Poisson distribution itself, see Tables 5.1 and 5.2. We only need to specify the probability above λt , for example, 0.9. For large λ , 50% of the distribution will be below λt . With $\lambda < 1$ this is no longer the case.

This raises two questions which will be answered throughout this Master Thesis:

1. **Rate:** If T is fixed, what does the expected rate λ need to be to achieve a certain certainty of enrolling the total sample size N within the time frame T ?
2. **Time:** Given a certain rate λ , how long should the recruitment period T be planned to give a confidence above 50% of recruiting the total sample size N ? In Machine Learning, this confidence is aimed at 80%. In Carter (2004), at 90%.

5.4 Counts: Comparison exact vs Monte Carlo simulations

Carter raises two important questions, enumerated in the previous section (Carter, 2004; Carter et al., 2005). He suggests the use of Monte Carlo (MC) simulations for counts. Here we investigate the accuracy of his MC simulations by comparing them with exact distributions for accrual of counts introduced in Chapter 3.

As we saw in the previous chapter we can model the counts taking into account only the aleatory uncertainty using $C(Ttarget) \sim \text{Po}(\lambda Ttarget)$ with $Ttarget = 548$. Or, more realistically, take into consideration the fluctuation of Λ over time using $C(Ttarget) \sim \text{Po}(\Lambda Ttarget)$ with $\Lambda \sim G(\alpha, \beta)$.

Figures 5.1 and 5.2 show the comparison between the theoretical models for counts discussed in Chapter 3 and their respective MC simulations. In Figures 5.1 and 5.2, we can see how we need at least $M = 10^4$ MC results of simulations to converge to the theoretical probability distribution discussed in Chapter 3. Carter (2004) uses $M = 10^3$.

```
set.seed(2025)

M <- 10^4
Ttarget <- 548
t <- seq(1, Ttarget, 1)
lambda <- 0.591

cval_cum_matrix <- matrix(NA, nrow = M, ncol = length(t))

for (i in 1:M) {
  cval <- rpois(length(t), lambda)
  cval_cum_matrix[i, ] <- cumsum(cval)
}

final_counts <- cval_cum_matrix[, length(t)]
```

In Table 5.1 we illustrate how, indeed, by using the expected accrual without taking into consideration any uncertainty we have roughly a 50% chance of accruing the desired sample size in the established time-frame (Carter, 2004).

5.5 Time: Comparison exact vs Monte Carlo simulations

As we saw in Chapter 4 we can model the waiting time to accrue $Ctarget = 324$ objects when unit-time recruitment rate is $\lambda = 0.591$ taking into account only aleatory uncertainty with

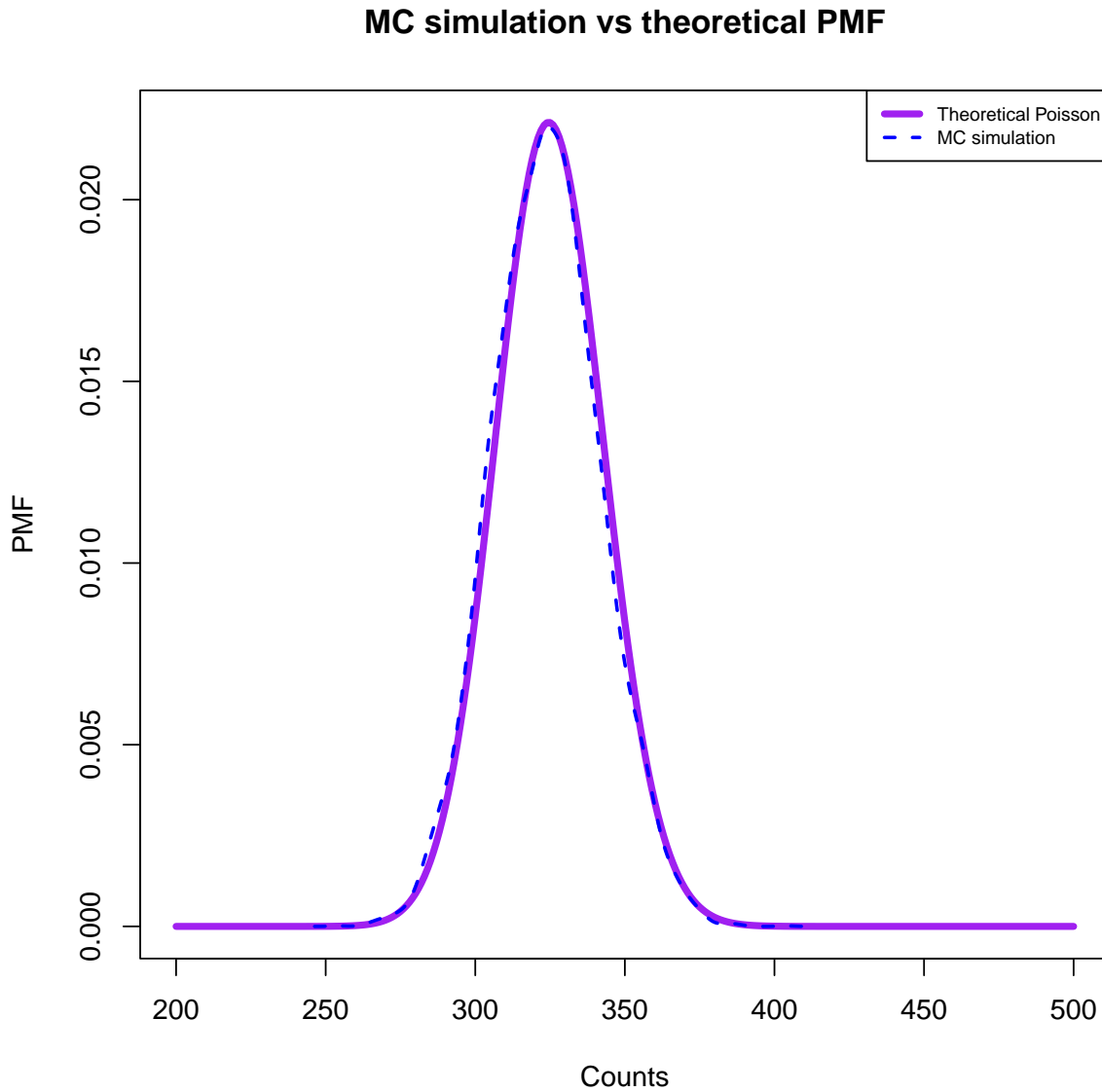


Figure 5.1: Comparison of smoothed theoretical Probability Mass Function (PMF) of Poisson model for counts with $\lambda = 0.591$ for accrual at time $T_{target} = 548$ and Monte Carlo (MC) simulations with $M = 10^4$.

Model	Estimated Probability	MCse	Exact Probability
$C(T_{target}) \sim \text{Po}(\lambda T_{target})$	$P(C(T_{target}) \geq 324) = 0.479$	0.005	0.508
$C(T_{target}) \sim \text{PoG}(T_{target}, \alpha, \beta)$	$P(C(T_{target}) \geq 324) = 0.48$	0.005	0.501

Table 5.1: Probability estimates based on Monte Carlo simulations, their respective Monte Carlo standard errors (MCse) and exact probability computations for processes considered in modeling counts where the waiting time is fixed as $T_{target} = 548$, $\lambda = 0.591$, $\alpha = 32.4$ and $\beta = 54.8$.

$T(C_{target}) \sim \text{Erlang}(C_{target}, \lambda)$. Or, taking into account both aleatory and epistemic uncertainty with $T(C_{target}) \sim \text{G}(C_{target}, \Lambda)$ where $\Lambda \sim \text{G}(\alpha, \beta)$.

Figures 5.3 and 5.4 show the comparison between the theoretical models for waiting time

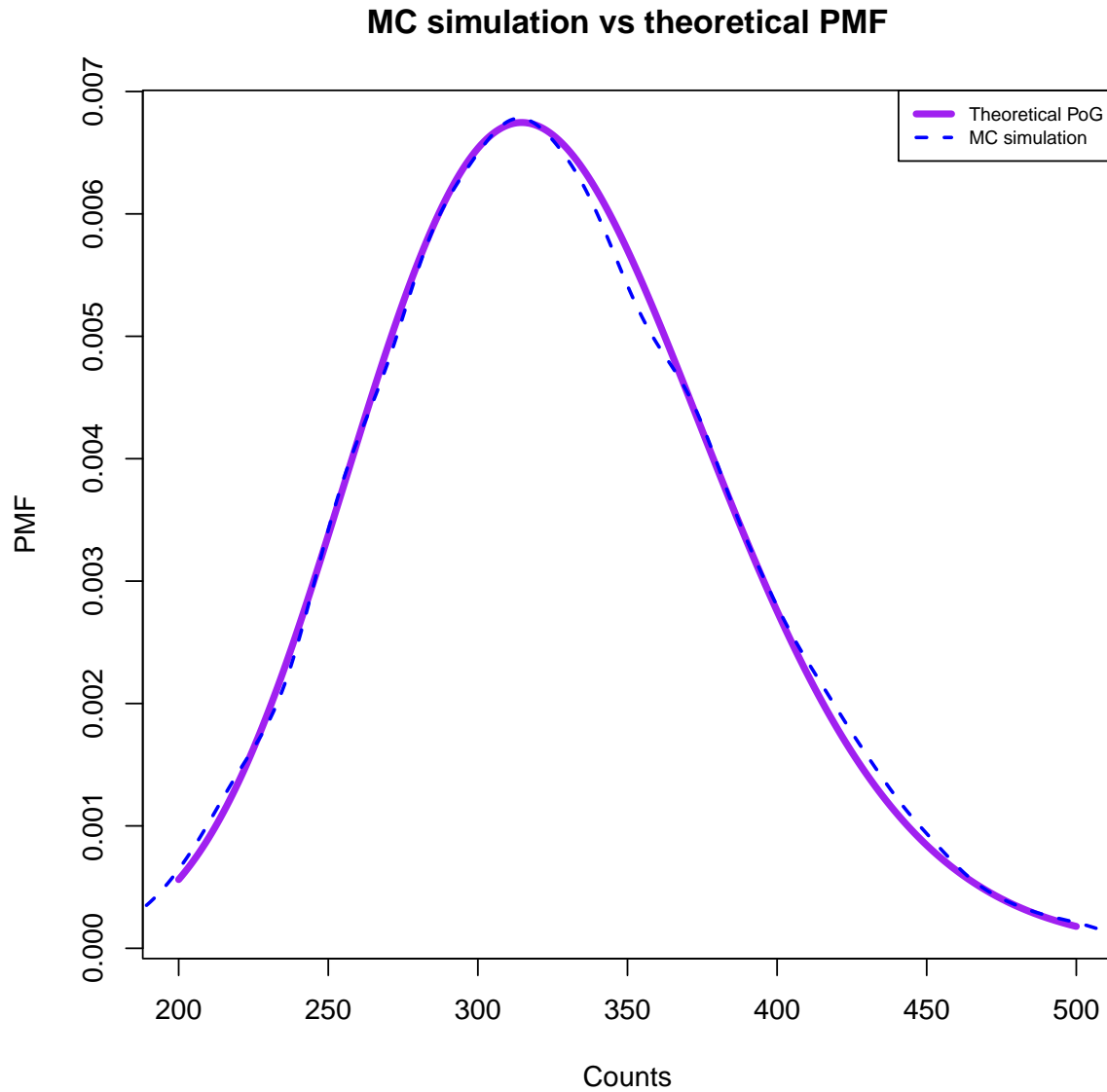


Figure 5.2: Comparison of smoothed theoretical Probability Mass Function (PMF) of Poisson-Gamma model for counts with $\alpha = 32.4$ and $\beta = 54.8$ for accrual at time $T_{target} = 548$, and Monte Carlo (MC) simulations with $M = 10^4$.

discussed in Chapter 4 and their respective MC simulations. In Figures 5.3 and 5.4, we can see how we need at least $M = 10^4$ MC results of simulations converge to the theoretical probability distribution discussed in Chapter 4.

In the following chunk of code we show [Carter \(2004\)](#) approach:

```
set.seed(2025)
M <- 10^4
Ctarget <- 324
Ttarget <- 548
lambda <- 0.591
t <- seq(1, Ttarget, 1)
```

```

timep <- rep(0, M)
csump <- rep(0, M)

for(m in 1:M){
  while (csump[m] < Ctarget) {
    csump[m] <- csump[m] + rpois(1, lambda)
    timep[m] <- timep[m] + 1
  }
}

```

However, a more efficient version was used for the MC simulations shown alongside the adaptations for the Gamma-Gamma model.

```

M <- 10^4
Ctarget <- 324
lambda <- 0.591

alpha <- 32.4
beta <- 54.8

simulate_time_to_threshold_Erlang <- function(MM, CC, ll, rseed=265735) {
  set.seed(rseed)
  timeerlang <- rgamma(n=MM, shape = CC, rate = ll)
  return(timeerlang)
}

time_erlang <- simulate_time_to_threshold_Erlang(MM=M, CC=Ctarget, ll=lambda, rseed=265735)

simulate_time_to_threshold_GG <- function(MM, CC, aa, bb, rseed=265735) {
  set.seed(rseed)
  timeegg <- rep(0, MM)
  lambdar <- rgamma(n=MM, shape = aa, rate = bb)
  for (i in 1:MM){
    timeegg[i] <- rgamma(n=1, shape = CC, rate = lambdar[i])
  }
  return(timeegg)
}

timeegg <- simulate_time_to_threshold_GG(MM=M, CC=Ctarget, aa=alpha, bb=beta)

```

Model	Estimated Probability	MCse	Exact Probability
$T(Ctarget) \sim G(Ctarget, \lambda)$	$P(T(Ctarget) \geq 548) = 0.498$	0.005	0.496
$T(Ctarget) \sim GG(Ctarget, \alpha, \beta)$	$P(T(Ctarget) \geq 548) = 0.52$	0.005	0.52

Table 5.2: Probability estimates based on Monte Carlo simulations, their respective Monte Carlo standard errors (MCse) and exact probability computations for all processes considered in modeling time where the sample size is fixed to be $Ctarget = 324$, $\lambda = 0.591$, $\alpha = 32.4$ and $\beta = 54.8$.

Small number of simulations (up to $M = 10^3$) from [Carter \(2004\)](#) gives him inaccurate

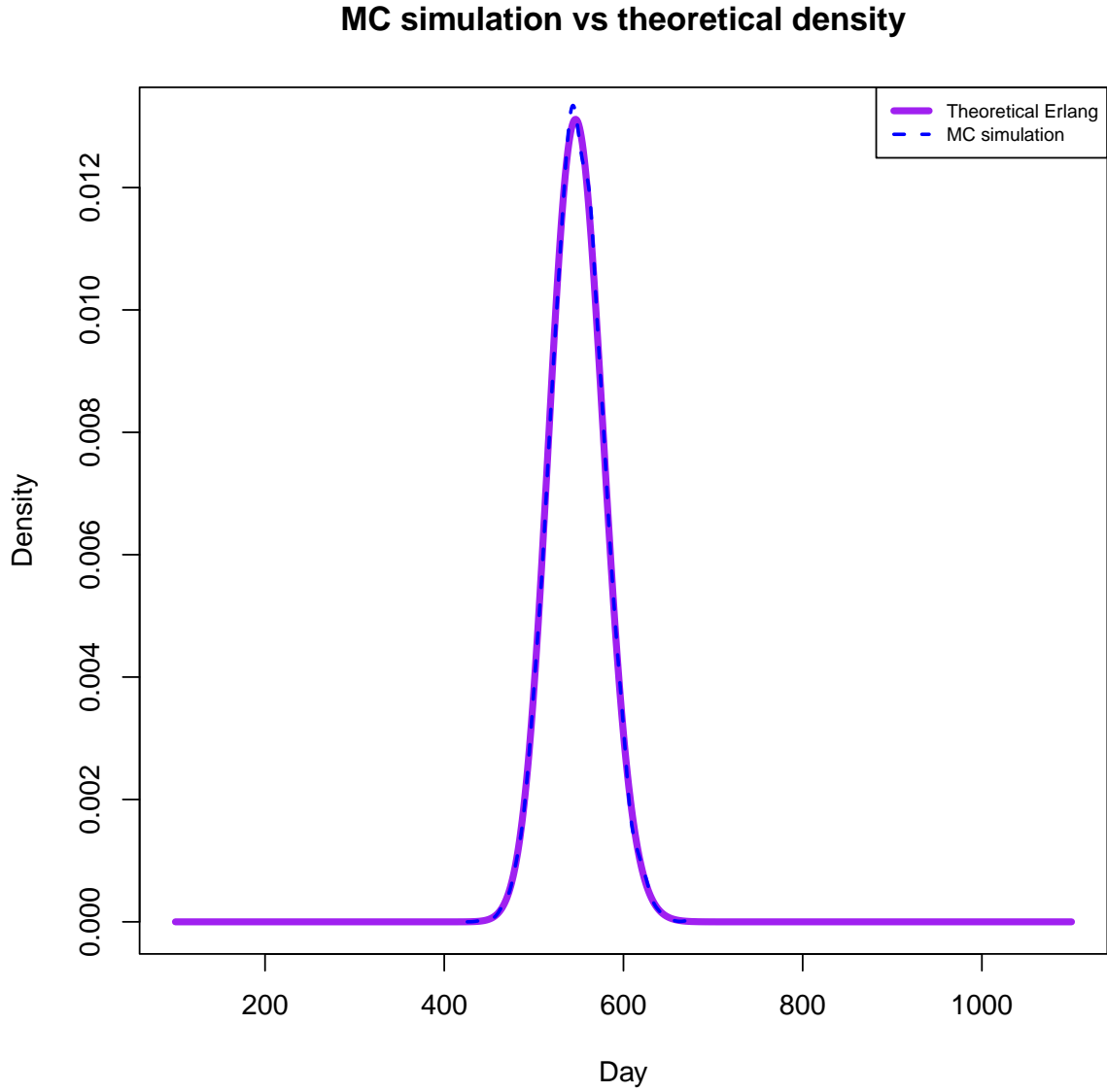


Figure 5.3: Comparison of theoretical density function of Erlang model for the waiting time until $C_{target} = 324$ subjects are accrued with recruitment rate $\lambda = 0.591$ and Monte Carlo (MC) simulations with $M = 10^4$.

estimate of days (580), when the exact using the Erlang distribution gives 588 to have 90% chance of accruing $C_{target} = 324$ subjects with a recruitment rate of $\lambda = 0.591$.

Moreover, if we wish to be more realistic in the uncertainty our model takes into consideration and choose the Gamma-Gamma distribution, 707 days would be required to have a 90% chance of accruing the desired sample size, see Figure 5.5.

In Table 5.2 we illustrate how, indeed, by using the expected accrual without taking into consideration any uncertainty we have roughly a 50% chance of accruing the desired sample size in the established time-frame (Carter, 2004).

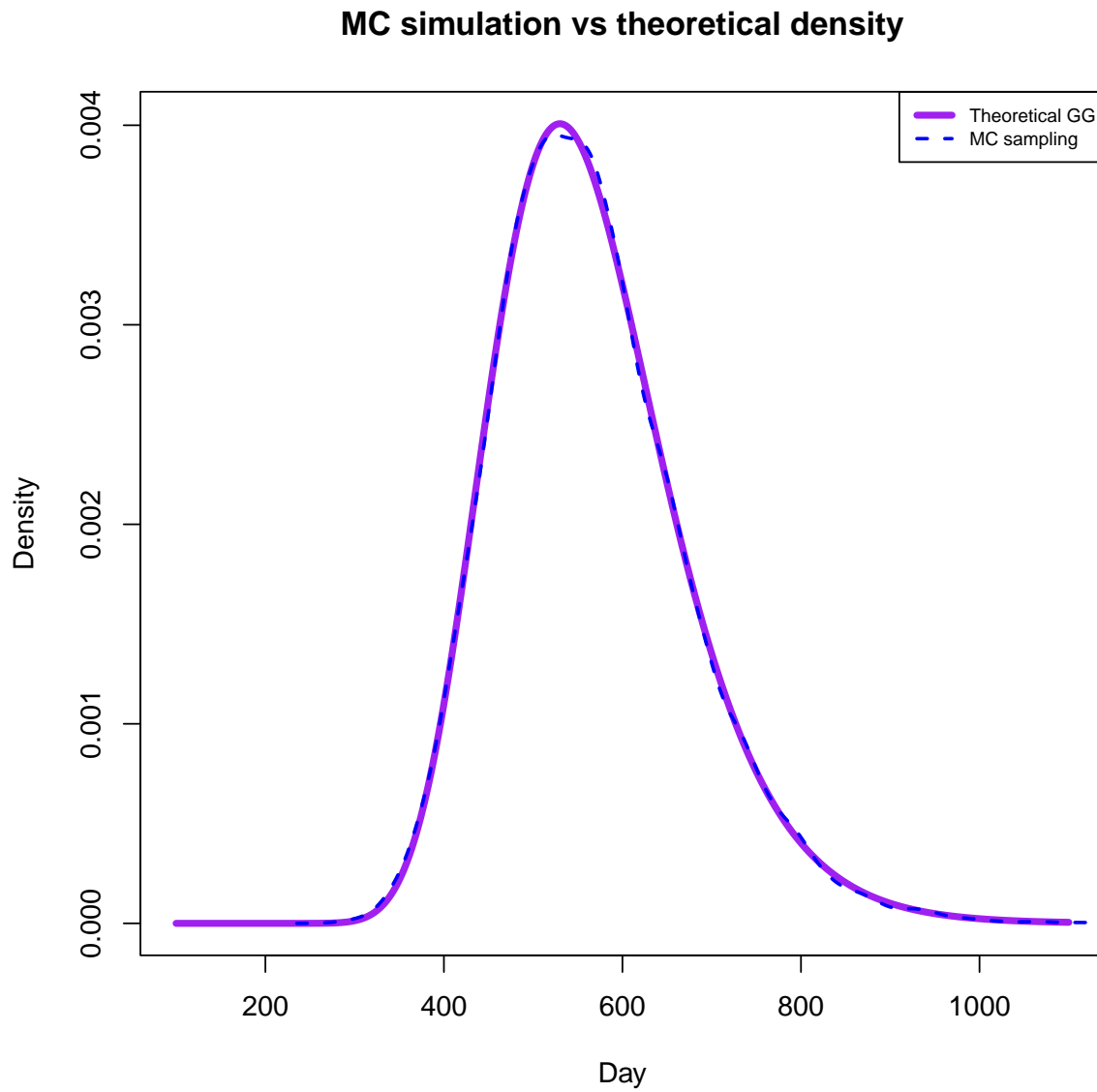


Figure 5.4: Comparison of theoretical density function of Gamma-Gamma model for waiting time with parameters $C_{target} = 324$, $\alpha = 32.4$ and $\beta = 54.8$ and Monte Carlo (MC) simulations with $M = 10^4$.

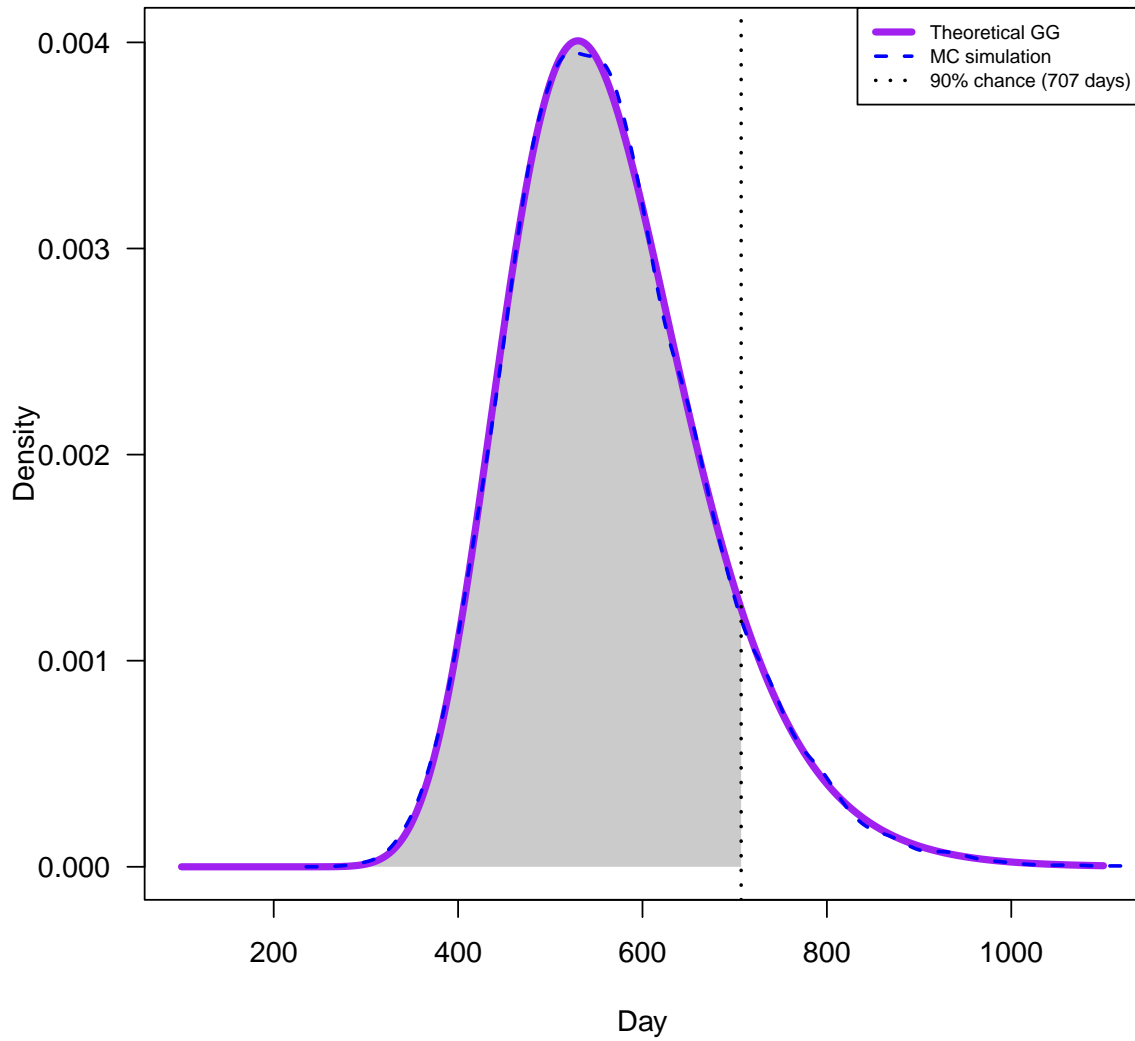


Figure 5.5: Illustration showing that, under a theoretical Gamma-Gamma model with parameters $\alpha = 32.4$ and $\beta = 54.8$, it takes approximately 707 days to reach a 90% probability of achieving the target sample size ($C_{\text{target}} = 324$).

Chapter 6

Discussion

A comprehensive graphical representation of study flow and recruitment at each stage of a clinical trial, including points of participant leakage, provides valuable insights into trial dynamics. Visual depictions of the accrual process, waiting times, and simulated accrual patterns across a hundred studies help clarify the complexities involved in participant recruitment and trial progression ([Spiegelhalter *et al.*, 2011](#)). These visual tools not only aid in the interpretation of recruitment efficiency but also highlight the importance of taking into consideration the uncertainty when planning a study at the design stage of a clinical trial.

Unified mathematical notation for theoretical models of counts and time has been developed to facilitate consistent analysis across the different scenarios ([Anisimov and Fedorov, 2007](#)). This notation allowed for the derivation of exact mathematical properties, including the expectation and variance, of the underlying distributions in both time and count models.

We extended the Monte Carlo simulation approach for count data and waiting times introduced by [Carter \(2004\)](#) to accommodate exact distributions. This extension enables the representation of aleatory uncertainty via the Poisson model for counts and the Erlang model for waiting times, as well as both aleatory and epistemic uncertainty through the Poisson-Gamma model for counts and the Gamma-Gamma model for waiting times ([O’Hagan, 2006](#); [Anisimov and Fedorov, 2007](#)). For comparison, we also include a deterministic model based solely on expected values, which does not account for uncertainty in either framework.

In the results section, we applied the exact theoretical methods to a real-world example drawn from [Carter \(2004\)](#), and compared the outcomes of Carter’s Monte Carlo simulations with those obtained using our exact approach. While we recommend the use of exact methods whenever feasible due to their precision and analytical rigor, we note that Monte Carlo simulations can approximate the exact results closely when the number of simulations is sufficiently large (e.g. $M = 10^5$).

We explored two distinct approaches for generating fluctuating recruitment rates. In Version 1, the rate is fixed over time but varies across studies, while in Version 2, the rate varies both over time and across studies. These two versions differ not only empirically, as demonstrated through Monte Carlo simulations, but also theoretically, with derivations provided for both count and time models. Throughout this project, all methods were implemented using Version 1; however, the framework can be extended to accommodate time-varying rates as in Version 2.

Sensitivity analyses were conducted for both the count and time models, revealing that decreasing certain parameters increases the uncertainty of the models. Moreover, a link to open-source R software necessary to replicate this Master Thesis was provided in [Appendix A](#).

This project has several limitations that present opportunities for future research. First, our analysis was limited to point estimates and a narrow set of distributions: Poisson, Poisson-Gamma, Erlang, and Gamma-Gamma. It would be valuable to consider other likelihoods, such as the Weibull or normal distributions, which may better suit different types of data. Second, we analyzed the study as a whole and did not account for possible variation across recruiting

centers. Introducing center-specific analyses could provide more detailed insights. Lastly, the model parameters were taken directly from the practical example in [Carter \(2004\)](#), without a formal elicitation process. A natural extension would involve developing methods to elicit prior information more systematically.

We addressed the questions provided by [Carter \(2004\)](#), regarding recruitment rate and waiting time based on Monte Carlo simulation. If we fix the time, what recruitment rate do we need to recruit the required sample size? And, in turn, if we fix our rate, how long should the recruitment period be to achieve the required sample size with a confidence of at least 80%? To this end, we elaborated the exact theoretical distributions that allow us to answer these questions and are a clear extension of [Carter \(2004\)](#) methods. We thus consolidated faster, more reliable exact methods that can be used at the design stage of a study to predict accrued counts and waiting time at each stage indicated by [Figure 2.1](#). Open-source R software is available and provided in [Appendix A](#) to apply this methods in practice.

Appendix A

Reproducibility

A.1 Code Availability

The code to reproduce this Master Thesis along with README.md files to compile the report itself are publicly available on <https://github.com/ppasto/masterthesis#>.

A.2 Personal Statement

This thesis was not written by any generative AI. It was written independently and without assistance from third parties. All sources utilized in this thesis are appropriately cited in the references

A.3 Session Info

`sessionInfo()`

```
sessionInfo()
## R version 4.4.2 (2024-10-31)
## Platform: x86_64-apple-darwin20
## Running under: macOS Sonoma 14.7.4
##
## Matrix products: default
## BLAS: /System/Library/Frameworks/Accelerate.framework/Versions/A/Frameworks/vecLib.framework/Versions/A/libBLAS.dylib
## LAPACK: /Library/Frameworks/R.framework/Versions/4.4-x86_64/Resources/lib/libRlapack.dylib; LAPACK version 3.12.0
##
## locale:
## [1] en_US.UTF-8/en_US.UTF-8/en_US.UTF-8/C/en_US.UTF-8/en_US.UTF-8
##
## time zone: Europe/Zurich
## tzcode source: internal
##
## attached base packages:
## [1] stats      graphics  grDevices  utils      datasets  methods   base
##
## other attached packages:
## [1] MASS_7.3-61      tidyr_1.3.1      dplyr_1.1.4      ggExtra_0.10.1
## [5] ggplot2_3.5.1    knitr_1.49
##
## loaded via a namespace (and not attached):
## [1] gtable_0.3.6      miniUI_0.1.1.1    compiler_4.4.2
## [4] highr_0.11        promises_1.3.2    tidyselect_1.2.1
## [7] Rcpp_1.0.14       later_1.4.1       scales_1.3.0
## [10] fastmap_1.2.0     mime_0.12         R6_2.5.1
## [13] generics_0.1.3    tibble_3.2.1      munsell_0.5.1
## [16] shiny_1.10.0      pillar_1.10.1     rlang_1.1.4
## [19] httpuv_1.6.15     xfun_0.50         cli_3.6.3
## [22] withr_3.0.2       magrittr_2.0.3    digest_0.6.37
```

```
## [25] grid_4.4.2          rstudioapi_0.17.1 xtable_1.8-4
## [28] lifecycle_1.0.4     vctrs_0.6.5        evaluate_1.0.3
## [31] glue_1.8.0          codetools_0.2-20    colorspace_2.1-1
## [34] purrr_1.0.2         tools_4.4.2         pkgconfig_2.0.3
## [37] htmltools_0.5.8.1
```

Bibliography

- Anisimov, V. V. and Fedorov, V. V. (2007). Modelling, prediction and adaptive adjustment of recruitment in multicentre trials. *Statistics in Medicine*, **26**, 4958–4975. [3](#), [11](#), [41](#)
- Bagiella, E. and Heitjan, D. F. (2001). Predicting analysis times in randomized clinical trials. *Statistics in Medicine*, **20**, 2055–2063. [3](#), [12](#), [27](#)
- Barnard, K. D., Dent, L., and Cook, A. (2010). A systematic review of models to predict recruitment to multicentre clinical trials. *BMC Medical Research Methodology*, **10**, 1–8. [9](#)
- Bogin, V. (2022). Lasagna’s law: A dish best served early. *Contemporary Clinical Trials Communications*, **26**, 100900. [6](#), [8](#)
- Carter, R. E. (2004). Application of stochastic processes to participant recruitment in clinical trials. *Controlled Clinical Trials*, **25**, 429–436. [3](#), [9](#), [10](#), [11](#), [29](#), [33](#), [34](#), [36](#), [37](#), [38](#), [41](#), [42](#)
- Carter, R. E., Sonne, S. C., and Brady, K. T. (2005). Practical considerations for estimating clinical trial accrual periods: application to a multi-center effectiveness study. *BMC Medical Research Methodology*, **5**, 1–5. [9](#), [10](#), [11](#), [34](#)
- Comfort, S. (2013). Improving clinical trial enrollment forecasts using sorm. *MJH Life Sciences*, **22**, . [9](#)
- Desai, R. (2014). *Preventing Patient Volume Leakage in Healthcare Systems*. PhD thesis, University of Pittsburgh. [3](#), [6](#)
- Food, Administration, D., *et al.* (2018). Evaluating inclusion and exclusion criteria in clinical trials. In *Workshop Report. The National Press Club, Washington DC*. [5](#)
- Frank, G. (2004). Current challenges in clinical trial patient recruitment and enrollment. *SoCRA Source*, **2**, 30–38. [5](#)
- Held, L. and Bové, D. S. (2014). *Applied Statistical Inference*. Springer. [10](#), [14](#), [16](#), [20](#), [25](#), [28](#), [33](#)
- Hilbe, J. M. (2011). *Negative Binomial Regression*. Cambridge University Press. [16](#)
- Hopewell, S., Chan, A.-W., Collins, G. S., Schultz, K. F., *et al.* (2025). Consort 2025 statement: updated guideline for reporting randomised trials. *The Lancet*, **405**, 1633–1640. [3](#), [5](#), [7](#)
- Johnson, N. L., Kemp, A. W., and Kotz, S. (2005). *Univariate Discrete Distributions*. John Wiley & Sons. [14](#), [16](#)
- Lim, C.-Y. and In, J. (2019). Randomization in clinical studies. *Korean Journal of Anesthesiology*, **72**, 221–232. [5](#)
- Liu, J., Jiang, Y., Wu, C., Simon, S., Mayo, M. S., Raghavan, R., and Gajewski, B. J. (2023). *accrual: Bayesian Accrual Prediction*. R package version 1.4. [11](#), [17](#), [21](#), [22](#), [23](#), [24](#), [31](#), [32](#)

- Meeker, W. Q., Hahn, G. J., and Escobar, L. A. (2017). *Statistical Intervals: A Guide for Practitioners and Researchers*. John Wiley & Sons. 15
- Mountain, R. and Sherlock, C. (2022). Recruitment prediction for multicenter clinical trials based on a hierarchical poisson–gamma model: Asymptotic analysis and improved intervals. *Biometrics*, **78**, 636–648. 11
- National Institute of Allergy and Infectious Diseases (2021). Screening, enrollment, and unblinding of participants. <https://www.niaid.nih.gov/sites/default/files/screening-enrollment-unblinding-of-participants.pdf>. Accessed: 2025-02-10. 5
- Nüesch, E., Trelle, S., Reichenbach, S., Rutjes, A. W., Bürgi, E., Scherer, M., Altman, D. G., and Jüni, P. (2009). The effects of excluding patients from the analysis in randomised controlled trials: meta-epidemiological study. *BMJ*, **339**, 1–7. 5
- O’Hagan, A. e. a. (2006). *Uncertain Judgements: Eliciting Experts’ Probabilities*. John Wiley & Sons. 3, 6, 41
- Panos, G. D. and Boeckler, F. M. (2023). Statistical analysis in clinical and experimental medical research: Simplified guidance for authors and reviewers. 3, 5
- Piantadosi, S. (2024). *Clinical Trials: A Methodologic Perspective*. John Wiley & Sons. 6
- Piantadosi, S. and Meinert, C. L. (2022). *Principles and Practice of Clinical Trials*. Springer Nature. 6, 8
- R Core Team (2024). *The ‘stats’ Package: R Base Package for Statistical Functions*. R Foundation for Statistical Computing, Vienna, Austria. R package version X.Y.Z. 15
- Rehman, A. M., Ferrand, R., Allen, E., Simms, V., McHugh, G., and Weiss, H. A. (2020). Exclusion of enrolled participants in randomised controlled trials: what to do with ineligible participants? *BMJ Open*, **10**, e039546. 5
- Schulz, K. F., Altman, D. G., and Moher, D. (2010). Consort 2010 statement: updated guidelines for reporting parallel group randomised trials. *Journal of Pharmacology and Pharmacotherapeutics*, **1**, 100–107. 3, 5, 7
- Shih, W. J. (2002). Problems in dealing with missing data and informative censoring in clinical trials. *Current Controlled Trials in Cardiovascular Medicine*, **3**, 1–7. 5
- Spiegelhalter, D., Pearson, M., and Short, I. (2011). Visualizing uncertainty about the future. *Science*, **333**, 1393–1400. 11, 14, 17, 18, 21, 22, 23, 24, 31, 32, 41
- Van Spall, H. G., Toren, A., Kiss, A., and Fowler, R. A. (2007). Eligibility criteria of randomized controlled trials published in high-impact general medical journals: A systematic sampling review. *JAMA*, **297**, 1233–1240. 5
- Whelan, J., Le Deley, M.-C., Dirksen, U., Le Teuff, G., Brennan, B., Gaspar, N., Hawkins, D. S., Amler, S., Bauer, S., Bielsack, S., *et al.* (2018). High-dose chemotherapy and blood autologous stem-cell rescue compared with standard chemotherapy in localized high-risk ewing sarcoma: Results of euro-ewing 99 and ewing-2008. *Journal of Clinical Oncology*, **36**, 3110–3119. 6, 7, 8
- White, D. and Hind, D. (2015). Projection of participant recruitment to primary care research: a qualitative study. *Trials*, **16**, 1–13. 27
- Willie, M. M. (2024). Population and target population in research methodology. *Golden Ratio of Social Science and Education*, **4**, 75–79. 5

- Zhang, X. and Long, Q. (2012). Modeling and prediction of subject accrual and event times in clinical trials: a systematic review. *Clinical Trials*, **9**, 681–688. [9](#)

